Table 4 SNP-43, Indel-19, and SNP-63 and type 2 diabetes in Japanese—a pooled analysis. The number of subjects of each genotype are indicated. All genotypic distributions are in Hardy-Weinberg equilibrium. The cases were divided into two groups based on the median age-at-diagnosis in the pooled sample—50 years. Note that age-at-diagnosis was not available for all subjects

Marker	Genotype	Overall			Age-at-diagnosis < 50 years		Age-at-diagnosis ≥50 years	
		Ctrl	T2D	*P*	T2D	*P*	T2D	*P*
SNP-43	G/G	833	811		255		276	
	G/A	91	104		28	0.98	32	0.78
	A/A	0	1	0.35	0		0	
	Allele frequency	G: 0.95	G: 0.94		G: 0.95		G: 0.95	
		A: 0.05	A: 0.06	0.25	A: 0.05	0.98	A: 0.05	0.79
Indel-19[a]	2R/2R	127	124		36		58	
	2R/3R	381	396		143		151	0.11
	3R/3R	334	316	0.67	107	0.33	105	
	Allele frequency	2R: 0.38	2R: 0.39		2R: 0.38		2R: 0.43	
		3R: 0.62	3R: 0.61	0.69	3R: 0.62	0.91	3R: 0.57	0.04
SNP-63	C/C	451	443		149		151	
	C/T	319	333		125		129	
	T/T	68	62	0.72	14	0.09	28	0.35
	Allele frequency	C: 0.73	C: 0.73		C: 0.73		C: 0.71	
		T: 0.27	T: 0.27	0.94	T: 0.27	0.79	T: 0.29	0.17

[a] Indel-19: 2R, 2 repeats of 32-bp sequence; 3R, 3 repeats

Table 5 CAPN10 haplotype frequency and risk of type 2 diabetes in Japanese—a pooled analysis. The haplotypes are those defined by SNP-43, Indel-19, and SNP-63, and the specific alleles are: SNP-43, allele 1, G and allele 2, A; Indel-19, allele 1, 2 repeats of 32-bp sequence, and allele 2, 3 repeats; and SNP-63, allele 1, C, and allele 2, T. The cases were divided into two groups based on the median age-at-diagnosis in the pooled sample—50 years. Note that age-at-diagnosis was not available for all subjects. *Ctrl* control, *T2D* type 2 diabetes

Haplotype	Overall				Age-at-diagnosis < 50 years			Age-at-diagnosis ≥50 years		
	Ctrl (n=825)	T2D (n=827)	OR (95% CI)[a]	*P*	T2D (n=277)	OR (95% CI)[a]	*P*	T2D (n=305)	OR (95% CI)[a]	*P*
111	0.106	0.113	1.07 (0.86–1.34)	0.52	0.117	1.12 (0.83–1.52)	0.46	0.136	1.33 (1.00–1.75)	0.05
121	0.572	0.553	0.93 (0.81–1.07)	0.29	0.567	0.98 (0.81–1.19)	0.85	0.515	0.80 (0.66–0.96)	0.02
112	0.270	0.274	1.02 (0.88–1.19)	0.79	0.265	0.98 (0.78–1.21)	0.82	0.297	1.14 (0.93–1.40)	0.21
221	0.052	0.059	1.15 (0.85–1.54)	0.37	0.051	0.97 (0.62–1.50)	0.88	0.052	1.01 (0.66–1.53)	0.97

[a] The OR and 95% CI of each haplotype relative to other haplotypes as a group are shown

Table 6 CAPN10 haplogenotype and risk of type 2 diabetes in Japanese—a pooled analysis. The haplotypes are those defined by SNP-43, Indel-19, and SNP-63, and the specific alleles are indicated in the legend to Table 5. The number of individuals with each haplogenotype is indicated

Haplogenotype	Overall				Age-at-diagnosis < 50 years			Age-at-diagnosis ≥ 50 years		
	Ctrl	T2D	OR (95% CI)[a]	*P*	T2D	OR (95% CI)[a]	*P*	T2D	OR (95% CI)[a]	*P*
111/111	15	18	1.20 (0.60–2.40)	0.60	5	0.99 (0.36–2.76)	0.99	10	1.83 (0.82–4.07)	0.14
111/121	97	93	0.95 (0.70–1.29)	0.74	31	0.95 (0.62–1.45)	0.80	37	1.04 (0.69–1.55)	0.86
111/112	44	44	1.00 (0.65–1.53)	0.99	18	1.23 (0.70–2.17)	0.47	20	1.25 (0.72–2.15)	0.43
111/221	4	14	3.53 (1.24–10.1)	0.02	6	4.54 (1.42–14.5)	0.01	6	4.12 (1.27–13.3)	0.02
112/112	66	62	0.93 (0.65–1.34)	0.70	13	0.57 (0.31–1.04)	0.06	27	1.12 (0.70–1.78)	0.64
112/121	247	254	1.04 (0.84–1.28)	0.73	90	1.13 (0.84–1.51)	0.43	97	1.09 (0.82–1.45)	0.55
112/221	23	32	1.40 (0.82–2.41)	0.22	13	1.72 (0.86–3.41)	0.12	10	1.18 (0.56–2.51)	0.66
121/121	270	259	0.94 (0.76–1.15)	0.54	92	1.02 (0.77–1.37)	0.88	82	0.76 (0.56–1.01)	0.06
121/221	59	50	0.84 (0.57–1.23)	0.37	9	0.44 (0.22–0.87)	0.02	16	0.72 (0.41–1.27)	0.25
221/221	0	1	–	–	0			0		

[a] The OR and 95% CI of each haplogenotype relative to the other haplotype combinations as a group are shown

Melander et al. 2002; Malecki et al. 2002) but at decreased risk in older Japanese raises the possibility that additional genetic variation may distinguish high- and low-risk subtypes of the 121 haplotype. Transpopulation mapping may be a useful strategy for identifying this variation.

Acknowledgements The authors thank Ms. A. Nogami, Ms. M. Y. Sagisaka, and Mr. M. Ikeda for their skillful technical assistance. This study was supported by Grants-in-Aid for Scientific Research C (10671084, 10470234) and for Scientific Research on Priority Areas Medical Genome Science from the Japan Ministry of Science, Education, Sports, Culture and Technology (12204102, 13204082, 14013059, 15012250), Novo Nordisk Foundation, the Naito Foundation (to N.I.) and Grants-in-Aid for Scientific Research B (13470223, 13557091) (to Y.H.), and U.S. Public Health Service (Grants DK-20595, −47486 and −55889). G.I.B. is an Investigator of the Howard Hughes Medical Institute.

References

Abecasis GR, Cookson WO (2000) GOLD–graphical overview of linkage disequilibrium. Bioinformatics 16:182–183

Baier LJ, Permana PA, Yang X, Pratley RE, Hanson RL, Shen GQ, Mott D, Knowler WC, Cox NJ, Horikawa Y, Oda N, Bell GI, Bogardus C (2000) A 1-10 gene polymorphism is associated with reduced muscle mRNA levels and insulin resistance. J Clin Invest 106:R69-R73

Daimon M, Oizumi T, Saitoh T, Kameda W, Yamaguchi H, Ohnuma H, Igarashi M, Manaka H, Kato T (2002) Calpain-10 gene polymorphisms are related, not to type 2 diabetes, but to increased serum cholesterol in Japanese. Diabetes Res Clin Pract 56:147–152

Horikawa Y, Oda N, Cox NJ, Li X, Orho-Melander M, Hara M, Hinokio Y, Lindner TH, Mashima H, Schwarz PE, del Bosque-Plata L, Oda Y, Yoshiuchi I, Colilla S, Polonsky KS, Wei S, Concannon P, Iwasaki N, Schulze J, Baier LJ, Bogardus C, Groop L, Boerwinkle E, Hanis CL, Bell GI (2000) Genetic variation in the gene encoding calpain-10 is associated with type 2 diabetes mellitus. Nat Genet 26:163–175

Horikawa Y, Oda N, Yu L, Imamura S, Fujiwara K, Makino M, Seino Y, Itoh M, Takeda J (2003) Genetic variations in calpain-10 gene are not a major factor in the occurrence of type 2 diabetes in Japanese. J Clin Endocrinol Metab 88:244–247

Iwasaki N, Cox NJ, Wang YQ, Schwarz PE, Bell GI, Honda M, Imura M, Ogata M, Saito M, Kamatani N, Iwamoto Y (2003) Mapping genes influencing type 2 diabetes risk and BMI in Japanese subjects. Diabetes 52:209–213

Johnson JD, Han Z, Otani K, Ye H, Zhang H, Wu H, Horikawa Y, Misler S, Bell GI, Polonsky KS (2004) RyR2 and calpain-10 delineate a novel apoptosis pathway in pancreatic islets. J Biol Chem 279:24794–24802

Malecki MT, Moczulski DK, Klupa T, Wanic K, Cyganek K, Frey J, Sieradzki J (2002) Homozygous combination of calpain 10 gene haplotypes is associated with type 2 diabetes mellitus in a Polish population. Eur J Endocrinol 146:695–699

Mori H, Ikegami H, Kawaguchi Y, Seino S, Yokoi N, Takeda J, Inoue I, Seino Y, Yasuda K, Hanafusa T, Yamagata K, Awata T, Kadowaki T, Hara K, Yamada N, Gotoda T, Iwasaki N, Iwamoto Y, Sanke T, Nanjo K, Oka Y, Matsutani A, Maeda E, Kasuga M (2001) The Pro12 → Ala substitution in PPAR-γ is associated with resistance to development of diabetes in the general population: possible involvement in impairment of insulin secretion in individuals with type 2 diabetes. Diabetes 50:891–894

Mori Y, Otabe S, Dina C, Yasuda K, Populaire C, Lecoeur C, Vatin V, Durand E, Hara K, Okada T, Tobe K, Boutin P, Kadowaki T, Froguel P (2002) Genome-wide search for type 2 diabetes in Japanese affected sib-pairs confirms susceptibility genes on 3q, 15q, and 20q and identifies two new candidate Loci on 7p and 11p. Diabetes 51:1247–1255

Orho-Melander M, Klannemark M, Svensson MK, Ridderstrale M, Lindgren CM, Groop L (2002) Variants in the calpain-10 gene predispose to insulin resistance and elevated free fatty acid levels. Diabetes 51:2658–2664

Seino S on behalf of the Study Group of Comprehensive Analysis of Genetic Factors in Diabetes Mellitus (2001) S20G mutation of the amylin gene is associated with Type II diabetes in Japanese. Diabetologia 44:906–909

Shima Y, Nakanishi K, Odawara M, Kobayashi T, Ohta H (2003) Association of the SNP-19 genotype 22 in the calpain-10 gene with elevated body mass index and hemoglobin A1c levels in Japanese. Clin Chim Acta 336:89–96

Song Y, Niu T, Manson JE, Kwiatkowski DJ, Liu S (2004) Are variants in the CAPN10 gene related to risk of type 2 diabetes? A quantitative assessment of population and family-based association studies. Am J Hum Genet 74:208–222

Weedon MN, Schwarz PE, Horikawa Y, Iwasaki N, Illig T, Holle R, Rathmann W, Selisko T, Schulze J, Owen KR, Evans J, Del Bosque-Plata L, Hitman G, Walker M, Levy JC, Sampson M, Bell GI, McCarthy MI, Hattersley AT, Frayling TM (2003) Meta-analysis and a large association study confirm a role for calpain-10 variation in type 2 diabetes susceptibility. Am J Hum Genet 73:1208–1212

Diabetologia (2005) 48: 336–344
DOI 10.1007/s00125-004-1636-8

ARTICLE

T. Sasaoka · K. Fukui · T. Wada · S. Murakami · J. Kawahara · H. Ishihara · M. Funaki · T. Asano · M. Kobayashi

Inhibition of endogenous SHIP2 ameliorates insulin resistance caused by chronic insulin treatment in 3T3-L1 adipocytes

Received: 28 April 2004 / Accepted: 4 September 2004 / Published online: 15 January 2005

Abstract *Aims/hypothesis:* SHIP2 is a physiologically important negative regulator of insulin signalling hydrolysing the PI3-kinase product, PI(3,4,5)P3, which also has an impact on insulin resistance. In the present study, we examined the effect of inhibiting the endogenous SHIP2 function on the insulin resistance caused by chronic insulin treatment. *Methods:* The endogenous function of SHIP2 was inhibited by expressing a catalytically inactive SHIP2 (ΔIP-SHIP), and compared with the effect of treatments designed to restore the levels of IRS-1 in insulin signalling systems of 3T3-L1 adipocytes. *Results:* Chronic insulin treatment induced the large (86%) down-regulation of IRS-1 and the modest (36%) up-regulation of SHIP2. Subsequent stimulation by insulin of Akt phosphorylation, PKCλ activity, and 2-deoxyglucose (2-DOG) uptake was markedly decreased by the chronic insulin treatment. Coincubation with the mTOR inhibitor, rapamycin, effectively inhibited the proteosomal degradation of IRS-1 caused by the chronic insulin treatment. Although the coincubation with rapamycin and advanced overexpression of IRS-1 effectively ameliorated subsequent insulin-induced phosphorylation of Akt, insulin stimulation of PKCλ activity and 2-DOG uptake was partly restored by these treatments. Similarly, expression of ΔIP-SHIP2 effectively ameliorated the insulin-induced phosphorylation of Akt without affecting the amount of IRS-1. Furthermore, the decreased insulin-induced PKCλ activity and 2-DOG uptake following chronic insulin treatment were ameliorated by the expression of ΔIP-SHIP2 more effectively than by the treatment with rapamycin. *Conclusions/interpretation:* Our results indicate that the inhibition of endogenous SHIP2 is effective in improving the state of insulin resistance caused by chronic insulin treatment.

Keywords Akt · Glucose uptake · Insulin · Insulin resistance · PKCλ · SHIP2

Abbreviations 2-DOG: 2-deoxyglucose · Glut4: glucose transporter 4 · IRS-1: insulin receptor substrate-1 · mTOR: mammalian target of rapamycin · PDGF: platelet-derived growth factor · PI3-kinase: phosphatidylinositol 3-kinase · PI(3,4)P2: phosphatidylinositol 3,4-bisphosphate · PI(3,4,5)P3: phosphatidylinositol 3,4,5-triphosphate · PKC: protein kinase C · SHIP2: SH2-containing inositol 5′-phosphatase 2

T. Sasaoka (✉)
Department of Clinical Pharmacology, Toyama Medical and Pharmaceutical University,
2630 Sugitani,
Toyama, 930-0194, Japan
e-mail: tsasaoka-tym@umin.ac.jp
Tel.: +81-76-4347551
Fax: +81-76-4345067

K. Fukui · T. Wada · S. Murakami · J. Kawahara · M. Kobayashi
First Department of Internal Medicine, Toyama Medical and Pharmaceutical University,
2630 Sugitani,
Toyama, 930-0194, Japan

H. Ishihara
Sainou Hospital,
Toyama, 930-0887, Japan

M. Funaki · T. Asano
Department of Internal Medicine, Graduate School of Medicine, University of Tokyo,
Tokyo, 113-8655, Japan

Introduction

The activation of phosphatidylinositol 3-kinase (PI3-kinase) is known to be important to the various metabolic actions of insulin [1–4]. PI(3,4,5)P3 produced by activated PI3-kinase is thought to function as a key lipid second messenger in insulin signalling to further downstream molecules [3–5]. We and others identified SH2-containing inositol 5′-phosphatase 2 (SHIP2) as a lipid phosphatase possessing 5′-phosphatase activity to hydrolyse PI(3,4,5)P3 to PI(3,4)P2 [6, 7]. Previous reports have indicated that overexpression of SHIP2 inhibits insulin-induced glucose uptake and glycogen synthesis via its 5′-phosphatase activity in 3T3-L1 adipocytes and L6 myocytes [8, 9]. Targeted

disruption of the SHIP2 gene in mice increased sensitivity to insulin without affecting other biological systems [10]. These findings indicate that SHIP2 is a physiologically important negative regulator that is relatively specific to insulin signalling. In addition, expression of SHIP2 protein is enhanced in the skeletal muscle and fat tissue of diabetic db/db mice [11]. Treatment with the insulin-senzsitizing thiazolidinedione, rosiglitazone, lowered the elevated levels of SHIP2 in the db/db mice [11]. Furthermore, a deletion in the 3′ untranslated region within the motifs implicated in the control of protein synthesis leading to the possible increase in expression of SHIP2 protein was identified in the UK and Belgian population of individuals with type 2 diabetes [12]. Therefore, SHIP2 is implicated in insulin resistance as a cause of type 2 diabetes in addition to the physiological importance in insulin signalling. Based on these findings, inhibition of endogenous SHIP2 function may be a target for ameliorating insulin signalling in the state of insulin resistance.

Hyperinsulinaemia is a hallmark of insulin resistance [13–15]. Chronic hyperinsulinaemia causes a desensitization to subsequent insulin responses, which appears to be part of the vicious cycle involved in the pathogenesis of type 2 diabetes [16–18]. In this regard, chronic treatment with insulin is known to facilitate the proteosomal degradation of IRS-1 leading to the down-regulation of insulin signalling at IRS-1 in 3T3-L1 adipocytes [17–19]. However, it is unknown whether SHIP2 is also involved in the resistance caused by chronic exposure to insulin. In the present study, the change in SHIP2 expression following chronic insulin treatment was investigated in 3T3-L1 adipocytes. In addition, the effect of inhibition of endogenous SHIP2 function using adenovirus-mediated gene transfer of a dominant-negative SHIP2 (ΔIP-SHIP2) on the possible amelioration of decreased insulin signalling caused by the chronic insulin treatment was investigated. The down-regulation of insulin signalling at the level of IRS-1 caused by the chronic insulin treatment can be ameliorated by pretreatment with rapamycin, which is an inhibitor of mTOR-dependent proteosomal degradation of IRS-1 [20, 21]. Alternatively, the decrease of IRS-1 can be prevented by overexpression of IRS-1 through adenovirus-mediated gene transfer [22]. Finally, the effects of the amelioration at the level of IRS-1 and SHIP2 on the chronic insulin treatment-induced down-regulation of insulin signalling were compared.

Materials and methods

Materials Human crystal insulin was provided by Novo Nordisk Pharmaceutical (Copenhagen, Denmark). [γ-^{32}P] ATP (111 TBq/mmol) and 2-[^{3}H]deoxyglucose (DOG; 3,330 GBq/mmol) were purchased from NEN Life Science Products (Boston, MA, USA). The two polyclonal anti-SHIP2 antibodies were described previously [7]. A polyclonal anti-PKCλ antibody was kindly provided by Dr W. Ogawa (Kobe University, Japan) [22]. A monoclonal anti-phosphotyrosine antibody (PY99) was from Transduction Laboratories (Lexington, KY, USA). A polyclonal anti-Thr^{308} phospho-specific Akt antibody, a polyclonal anti-Ser^{473} phospho-specific Akt antibody, and a monoclonal anti-PKCλ antibody were from Cell Signalling (Beverly, MA, USA). A polyclonal anti-Akt antibody and a polyclonal anti-Glut4 antibody were from Santa Cruz Biotechnology (Santa Cruz, CA, USA). A polyclonal IRS-1 antibody and a polyclonal anti-PDGF β receptor antibody were from Upstate Biotechnology (Lake Placid, NY, USA). Enhanced chemiluminescence reagents were from Amersham Pharmacia Biotech (Uppsala, Sweden). Dulbecco's modified Eagle's medium (DMEM), minimum essential medium (MEM) vitamin mixtures, and MEM amino acid solutions were from Gibco BRL Japan (Tokyo, Japan). All other reagents were of analytical grade and purchased from Sigma Chemical (St Louis, MO, USA) or Wako Pure Chemical Industries (Osaka, Japan).

Construction of adenoviral vectors A cDNA encoding a phosphatidylinositol 5′-phosphatase-defective mutant of SHIP2 (ΔIP-SHIP2) containing Pro^{687} to Ala, Asp^{691} to Ala, and Arg^{692} to Gly changes was subcloned into the vector pAxCAwt, and transferred to recombinant adenovirus by homologous recombination utilizing an Adenovirus Expression Vector Kit (Takara Biomedicals, Tokyo, Japan) as described previously [8]. The adenoviral vector encoding IRS-1 was also described previously [23].

Cell culture and infections with adenovirus 3T3-L1 fibroblasts were grown and passaged in DMEM supplemented with 10% donor calf serum. Cells at 2–3 days postconfluence were used for differentiation. The differentiation medium contained 10% fetal bovine serum (FBS), 250 nmol/l dexamethasone, 0.5 mmol/l isobutyl methylxanthine, and 500 nmol/l insulin. After 3 days, the differentiation medium was replaced with postdifferentiation medium containing 10% FBS and 500 nmol/l insulin. After 3 more days, the postdifferentiation medium was replaced with DMEM supplemented with 10% FBS. ΔIP-SHIP2 and IRS-1 were transiently expressed in differentiated 3T3-L1 adipocytes by means of adenovirus-mediated gene transfer. A multiplicity of infection (m.o.i.) of 10–40 pfu/cell was used to infect 3T3-L1 adipocytes in DMEM containing 2% FBS, with the virus being left on the cells for 16 h prior to removal. Subsequent experiments were conducted 24–48 h after initial addition of the virus [8]. The efficiency of adenovirus-mediated gene transfer of ΔIP-SHIP2 and IRS-1 was approximately 95%.

Measurements of PI(3,4,5)P3 and PI(3,4)P2 levels in vivo The same numbers of 3T3-L1 adipocytes transfected with LacZ or ΔIP-SHIP2 were starved of phosphate overnight in phosphate-free DMEM (Life Technology), then starved of serum for 3 h. [^{32}P]Orthophosphate (3.7 MBq/ml) was added, and the cells were cultured for an additional 2 h. Following the labelling period, the cells were incubated with or without 1 μmol/l insulin for 15 min. The reaction was terminated by washing once with ice-cold PBS, followed by the addition of methanol and 1 N HCl (1:1). The labelling of the cells with [^{32}P]orthophosphate was con-

ducted at the same time in both sets of transfected cells. Phospholipids were then extracted with chloroform. The extracted lipid was deacylated and subjected to amino-exchange high-performance liquid chromatography (HPLC) using a Partisphere strong anion-exchange column (Whatman) as described previously [8]. The PI(3,4)P2 and PI(3,4,5)P3 levels in the same sample for each line were measured within a single HPLC run. The radioactivity was detected with an online radiochemical detector.

Chronic insulin treatment 3T3-L1 adipocytes grown in 6-well multiplates were incubated with DMEM containing 0.1% FBS with or without 100 nmol/l insulin at 37°C for various periods. For experiments with rapamycin treatment, 20 nmol/l rapamycin was added for 30 min before the addition of insulin. At the end of the chronic treatment with insulin, the cells were washed with PBS, incubated in serum-free DMEM for 30 min, and washed again with PBS. The cells were then treated with or without 17 nmol/l insulin for 5 min.

Plasma membrane fractionation The cells were washed twice with PBS and once with HES buffer (255 mmol/l sucrose, 20 mmol/l HEPES, 1 mmol/l EDTA, 1 mmol/l phenylmethylsulphonyl fluoride [PMSF], 1 mmol/l Na_3VO_4, 2 μg/ml of aprotinin, and 50 ng/ml of okadaic acid, pH 7.4) and immediately homogenized by 20 strokes with a motor-driven homogenizer in HES buffer at 4°C. The homogenates (two 10-cm-diameter dishes per condition) were subjected to subcellular fractionation as described previously to isolate the plasma membrane (PM) [21]. In brief, the homogenates were centrifuged at 19,000 *g* for 20 min. The pellet obtained from the spin was resuspended in HES buffer, layered onto a 1.12 mol/l sucrose cushion, and centrifuged at 100,000 *g* in a swing rotor for 60 min. A white fluffy band at the interface was collected, resuspended in HES buffer, and centrifuged at 40,000 *g* for 20 min, yielding a pellet of PM. All fractions were adjusted to a final protein concentration of 1–3 mg/ml, which was measured by the Bradford method, and stored at −80°C until use.

Immunoprecipitation and western blotting The cells or the plasma membrane preparation were lysed in a buffer containing 20 mmol/l Tris, 150 mmol/l NaCl, 1 mmol/l EDTA, 1 mmol/l EGTA, 2.5 mmol/l sodium deoxycholate, 1 mmol/l β-glycerophosphate, 1% Triton X-100, 1 mmol/l PMSF, 1 mmol/l Na_3VO_4, 50 mmol/l sodium fluoride, 10 μg/ml of aprotinin, and 10 μmol/l leupeptin, pH 7.4, for 30 min at 4°C. The lysates were centrifuged to remove insoluble materials. The supernatants (100 μg of protein) were immunoprecipitated with antibodies for 2 h at 4°C. The precipitates or the lysates were then separated by 7.5% SDS-PAGE and transferred onto polyvinylidene difluoride membranes (PVDM) using a Bio-Rad Transblot apparatus. The membranes were blocked in a buffer containing 50 mmol/l Tris, 150 mmol/l NaCl, 0.1% Tween 20, and 2.5% bovine serum albumin (BSA) or 5% non-fat milk, pH 7.5, for 2 h at 20°C. They were then probed with antibodies for 2 h at 20°C or for 16 h at 4°C. After the membranes were washed in a buffer containing 50 mmol/l Tris, 150 mmol/l NaCl, and 0.1% Tween 20, pH 7.5, blots were incubated with a horseradish peroxidase-linked secondary antibody and subjected to enhanced chemiluminescence detection using ECL reagent according to the manufacturer's instructions (Amersham) [8]. In each experiment, the intensity of the band derived from control cells was assigned a value of 1 arbitrary unit, and the intensity of all treated groups was expressed as a fold value of control.

Measurement of PKCλ activity The cells were washed with ice-cold PBS and lysed with PKCλ buffer containing 50 mmol/l MOPS–HCl, 0.5% Triton X-100, 10% glycerol, 5 mmol/l EDTA, 5 mmol/l EGTA, 20 mmol/l NaF, 50 mmol/l β-glycerophosphate, 2 mmol/l Na_3VO_4, 2 mmol/l DTT, 1 μg/ml of leupeptin, and 2 mmol/l PMSF, pH 7.5. The lysates were centrifuged at 15,000 *g* for 20 min. The protein concentration in the resulting supernatants was determined with the use of bicinchoninic acid protein assay reagent (Pierce), and equal amounts of protein were subjected to immunoprecipitation with anti-PKCλ antibody. The immunoprecipitates were washed twice with PKCλ buffer containing 0.1% BSA, once with PKCλ buffer containing 0.1% BSA and 1 mol/l NaCl, and once with a solution containing 20 mmol/l Tris–HCl, 10% glycerol, 0.5 mmol/l EDTA, 0.5 mmol/l EGTA, 20 mmol/l 2-mercaptoethanol, 10 μg/ml of leupeptin, and 2 mmol/l PMSF, pH 7.5. Then, the precipitates were incubated for 14 min at 30°C with 14.8 kBq of [γ-^{32}ATP] in a reaction mixture (25 μl) containing 35 mmol/l Tris, pH 7.5, 10 mmol/l $MgCl_2$, 0.5 mmol/l EGTA, 0.1 mmol/l $CaCl_2$, 40 μmol/l unlabelled ATP, 100 μg/ml of phosphatidylserine, and 30 μmol/l myelin basic protein (MBP) as a substrate. Kinase reactions were terminated by the addition of SDS sample buffer, and the samples were then fractionated by SDS-PAGE [8, 22]. The radioactivity incorporated into substrates was determined with a Fuji BAS 2000 image analyser.

Measurement of 2-DOG uptake 3T3-L1 adipocytes grown in 6-well multiplates were serum-starved for 3 h. The cells were treated with or without rapamycin for 30 min and further incubated with 17 nmol/l insulin for 6 h. The cells were washed once with PBS, three times with Krebs–Ringer phosphate (KRP)–HEPES buffer, 10 nmol/l HEPES, 131.2 mmol/l NaCl, 4.7 mmol/l KCl, 1.2 mmol/l $MgSO_4$, 2.5 mmol/l $CaCl_2$, and 2.5 mmol/l NaH_2PO_4, pH 6.0, and once with KRP–HEPES buffer containing 1% BSA, pH 7.4. The cells were then incubated with the same KRP–HEPES buffer for 1 h at 37°C. The cells were subsequently stimulated with various concentrations of insulin. Following 15 min of insulin treatment, 3.7 kBq of 2-[^{3}H]DOG was added for 4 min. The reaction was stopped by the addition of 10 μmol/l cytochalasin B. The cells were washed three times with PBS and solubilized with 0.2 mmol/l SDS–0.2 N NaOH [8]. The radioactivity incorporated into the cells was measured by liquid scintillation counting.

Statistical analysis The data are represented as means ± SEM. p Values were determined using Student's t test, and $p<0.05$ was considered statistically significant.

Results

Effect of chronic insulin treatment on IRS-1 and SHIP2 Chronic treatment with insulin facilitates the proteosomal degradation of IRS-1 [20, 21, 24, 25]. Treatment with insulin reduced the amount of IRS-1, but not Akt, in a time-dependent manner in 3T3-L1 adipocytes. After 12 h of treatment, the amount of IRS-1 was 13.6±2.6% of the control level (Fig. 1a). In accordance with the reduced amount of IRS-1, the subsequent insulin-stimulated tyrosine phosphorylation of IRS-1 following chronic insulin treatment was markedly decreased to 13.2±1.8% (Fig. 1b). Thus, chronic insulin treatment caused an impairment of insulin signalling, at least, at the step involving IRS-1. Since SHIP2 is an important negative regulator of insulin signalling, alteration of its expression may cause insulin resistance [8–12]. In this regard, the amount of SHIP2 protein was relatively high after chronic treatment with insulin. Following 6 h of insulin treatment, the amount of SHIP2, but not Akt, was increased by 36.4±7.4% (Fig. 1c). Membrane targeting of SHIP2 is known to be important to its function to hydrolyse PI(3,4,5)P3 in insulin signalling [26]. The extent of insulin-induced translocation of SHIP2 to the plasma membrane fraction was increased by 33.4±8.3% compared to that without chronic insulin treatment. To assure equal amounts of protein were loaded among the samples, the PM fraction was immunoblotted with anti-PDGF β receptor antibody (Fig. 1d). These results indicate that chronic insulin treatment elicits insulin resistance, at least in part, at the level of SHIP2 as well as IRS-1.

Inhibition of endogenous SHIP2 function by expression of ΔIP-SHIP2 Because an elevated amount of SHIP2, especially at the plasma membrane, appears to be involved in the insulin resistance caused by the chronic insulin treat-

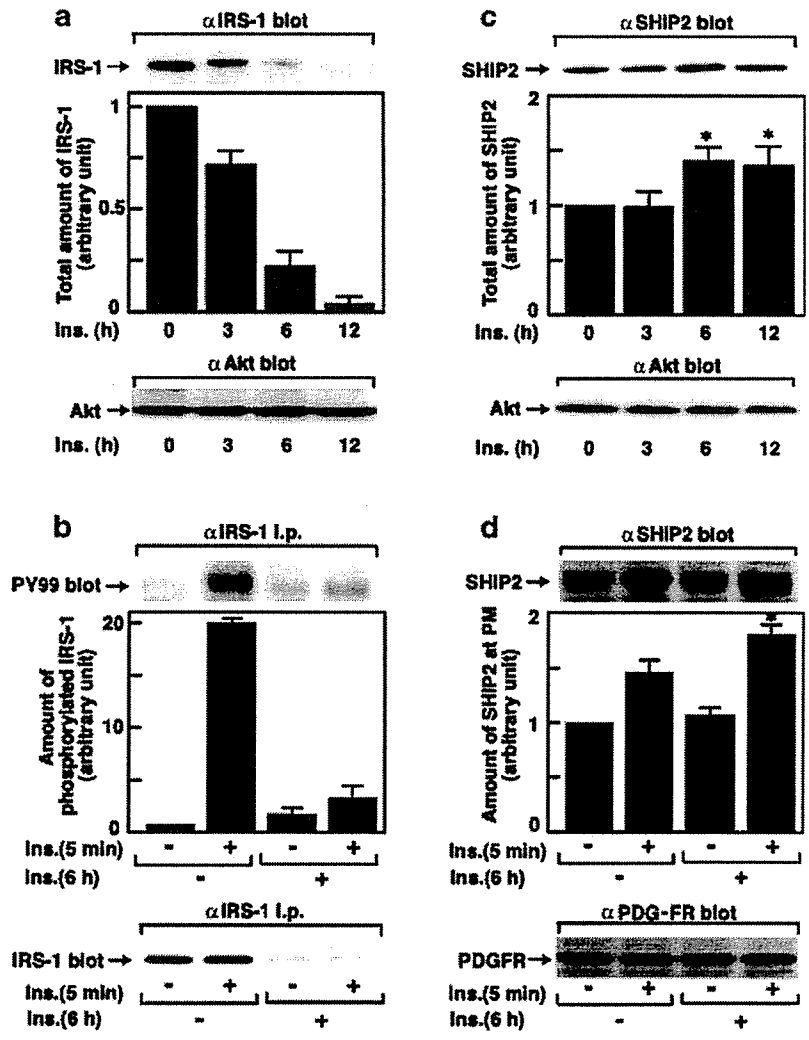

Fig. 1 Effect of chronic insulin treatment on IRS-1 and SHIP2. 3T3-L1 adipocytes were treated with 17 nmol/l insulin for the periods indicated (chronic insulin treatment). **a** The cells were lysed, and the proteins were separated by SDS-PAGE and immunoblotted with anti-IRS-1 antibody or anti-Akt antibody. **b** After chronic insulin treatment, the cells were washed with PBS and incubated in insulin-free medium for 30 min, then stimulated with 17 nmol/l insulin for 5 min (acute insulin treatment). The cell lysates were immunoprecipitated with anti-IRS-1 antibody. The precipitates were subjected to SDS-PAGE, and immunoblotted with anti-phosphotyrosine antibody (PY99) or anti-IRS-1 antibody. **c** The cell lysates were separated by SDS-PAGE and immunoblotted with anti-SHIP2 antibody or anti-Akt antibody. *$p<0.05$ versus amounts of SHIP2 without chronic insulin treatment. **d** The cells were homogenized and subjected to subcellular fractionation to yield the plasma membrane (PM) fraction. Samples in the PM fraction were separated by SDS-PAGE and immunoblotted with anti-SHIP2 antibody or anti-PDGF β receptor antibody. *$p<0.05$ versus amounts of SHIP2 at PM following 5 min of insulin stimulation without chronic insulin treatment. Results are means ± SEM of three separate experiments.

ment, expression of ΔIP-SHIP2, which acts in a dominant-negative manner, may ameliorate the impaired insulin signalling. Adenovirus-mediated gene transfer produced an eightfold increase in ΔIP-SHIP2 expression compared to the endogenous level of SHIP2 (Fig. 3b). The expression of ΔIP-SHIP2 increased insulin-induced generation of PI(3,4,5)P3, whereas the amount of PI(3,4)P2 was decreased (Fig. 2a). Thus, the expression of ΔIP-SHIP2 in fact functions to inhibit the endogenous 5′-phosphatase activity of SHIP2 in 3T3-L1 adipocytes. In addition, insulin-induced increase in the levels of PI(3,4,5)P3 was decreased to 25% after chronic insulin exposure. ΔIP-SHIP2 expression ameliorated the reduced levels of PI(3,4,5)P3 to 61% of the control level (data not shown). Thus, expression of ΔIP-SHIP2 appears to effectively ameliorate the decreased PI(3,4,5)P3 levels caused by chronic insulin treatment.

Effect of ΔIP-SHIP2 and IRS-1 expression, and pretreatment with rapamycin on insulin-induced phosphorylation of Akt after chronic insulin treatment Treatment with PI3-kinase inhibitor LY294002 effectively inhibited the chronic insulin treatment-induced degradation of IRS-1. Expression of ΔIP-SHIP2 partly abolished the inhibitory effect of LY294002 on the IRS-1 degradation, because SHIP2 is located downstream of PI3-kinase (data not shown). These results indicate that chronic insulin treatment induces the degradation of IRS-1 via PI3-kinase dependent mechanism. mTOR is a downstream molecule of PI3-kinase, and rapamycin is known to efficiently inhibit mTOR-dependent proteosomal degradation of IRS-1 in 3T3-L1 adipocytes [19–21]. Thus, the decrease in the amount of IRS-1 induced by degradation after chronic insulin treatment was effectively prevented by pretreatment with rapamycin. In contrast, expression of ΔIP-SHIP2 alone did not affect the loss of IRS-1 caused by the chronic insulin treatment. In addition, the preventive effect of rapamycin was not affected by the expression of ΔIP-SHIP2, because SHIP2 is located upstream of mTOR [8]. The decrease in IRS-1 caused by chronic insulin treatment can also be prevented by advanced overexpression of IRS-1. Thus, overexpression of IRS-1 in advance prevented the decrease in IRS-1 caused by chronic insulin treatment in an m.o.i.-dependent manner (data not shown). At an m.o.i. of 10 pfu/cell, the amount of IRS-1 after chronic insulin treatment was similar to that without chronic insulin treatment. The amount of protein loaded among the samples was confirmed to be identical by immunoblotting with anti-Akt antibody (Fig. 3b). As a result, rapamycin treatment and IRS-1 overexpression ameliorated the decreased levels of PI(3,4,5)P3 by chronic insulin treatment to 52% and 58%, respectively, of the control level (data not shown). Akt is an important mediator of the metabolic actions of insulin, and the activation of Akt is induced by the phosphorylation at Thr^{308} and Ser^{473} [8, 26–28]. Chronic insulin treatment decreased the subsequent insulin-stimulated phosphorylation of Akt at Thr^{308} and Ser^{473} to 23.8 ±2.0% and 28.5±2.1%, respectively. The reduction can be caused by the alteration of IRS-1 and/or SHIP2 following chronic insulin treatment. In this regard, pretreatment with rapamycin ameliorated the insulin-induced phosphorylation of Akt at Thr^{308} and Ser^{473}. Similarly, overexpression of ΔIP-SHIP2 effectively ameliorated the phosphorylation of Akt at Thr^{308} and Ser^{473} in an m.o.i.-dependent manner (data not shown), and it was most effectively ameliorated at an m.o.i. of 40 pfu/cell. The amelioration was more apparent and almost fully restored to the control level by both pretreatment with rapamycin and expression of ΔIP-SHIP2. In addition, the effective restoration of insulin-stimulated phosphorylation of Akt following chronic insulin treatment was also seen after advanced overexpression of IRS-1 (Fig. 3a).

Effect of ΔIP-SHIP2 and IRS-1 expression, and pretreatment with rapamycin, on insulin-induced activation of PKCλ after chronic insulin treatment Another important molecule downstream of PI3-kinase for metabolic insulin signalling is atypical PKC in 3T3-L1 adipocytes [22, 29]. In accordance with the results of insulin-induced phosphorylation of Akt, insulin stimulation of PKCλ activity was decreased to 23.8±3.9% of the control level after chronic insulin treatment. Pretreatment with rapamycin

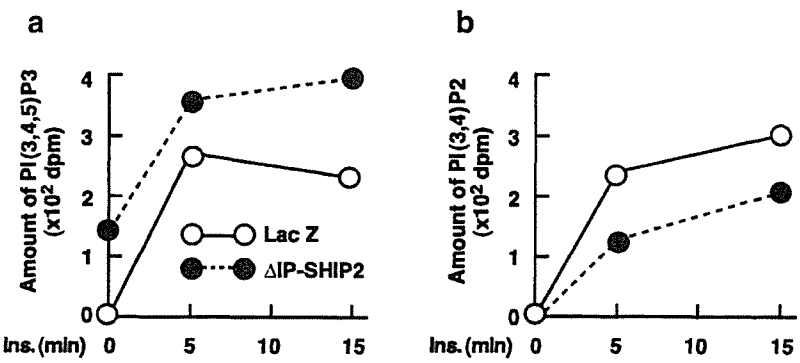

Fig. 2 Inhibition of endogenous SHIP2 function by expression of ΔIP-SHIP2. 3T3-L1 adipocytes were transfected with LacZ or ΔIP-SHIP2 at an m.o.i. of 40 pfu/cell. The cells were labelled with [^{32}P] orthophosphate for 2 h and incubated with or without insulin, and lipids were extracted with chloroform. The extracted lipids were analysed by HPLC after being deacylated. The amounts of ^{32}P-labelled PI(3,4,5)P3 (**a**) and PI(3,4)P2 (**b**) generated were determined with an online radiochemical detector. Results are means of two separate experiments.

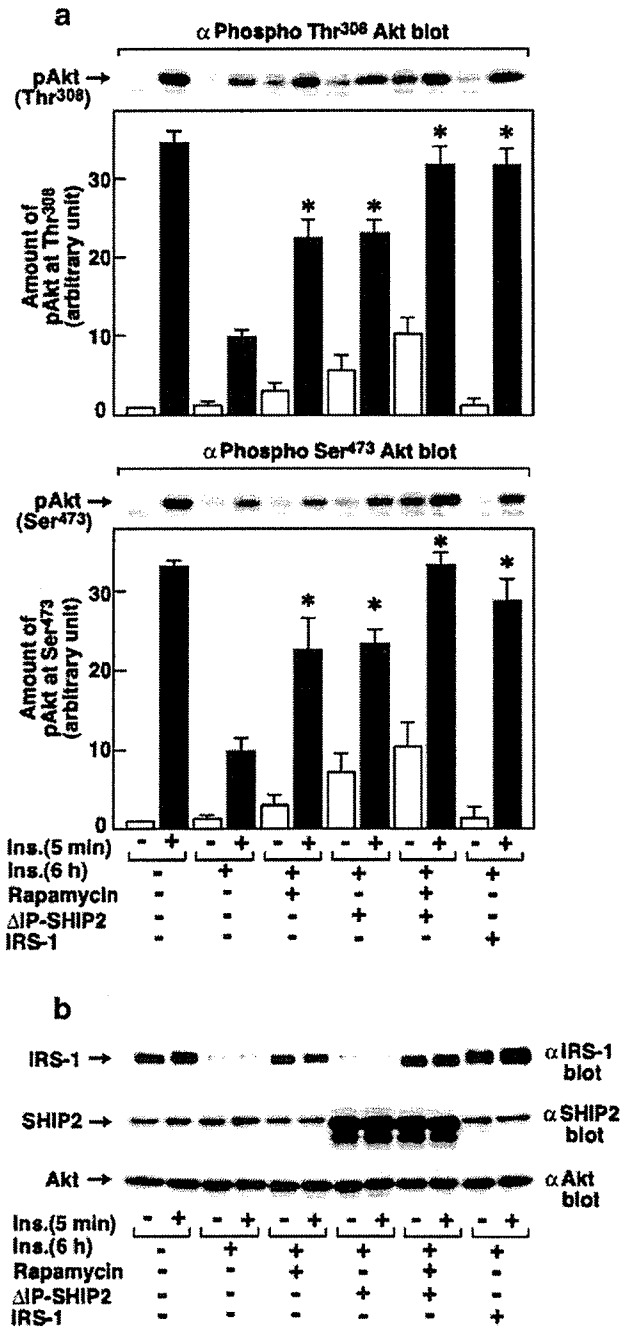

◀ **Fig. 3** Effect of ΔIP-SHIP2 and IRS-1 expression, and pretreatment with rapamycin on insulin-induced phosphorylation of Akt after chronic insulin treatment. 3T3-L1 adipocytes were transfected with LacZ and ΔIP-SHIP2 at an m.o.i of 40 pfu/cell, or IRS-1 at an m.o.i. of 10 pfu/cell. Serum-starved transfected cells were incubated with vehicle or 20 nmol/l rapamycin for 30 min, and treated with 17 nmol/l insulin for 6 h. The cells were washed with PBS and incubated in insulin-free medium for 30 min, and the cells were stimulated with 17 nmol/l insulin for 5 min. **a** The cells were lysed and the lysates were separated by SDS-PAGE and immunoblotted with anti-Ser^{473}-phospho-specific or anti-Thr^{308}-phospho-specific Akt antibody. The amount of Akt phosphorylated at Ser^{473} and Thr^{308} was quantitated by densitometry. Results are means ± SEM of four separate experiments. *$p<0.05$ versus amounts of phosphorylated Akt in LacZ-transfected cells with chronic insulin treatment. **b** The cell lysates were separated by SDS-PAGE, and immunoblotted with anti-IRS-1 antibody, anti-SHIP2 antibody, or anti-Akt antibody.

only partly restored the decreased PKCλ activity to 49.8± 3.8%. Although the effect was still partial, expression of ΔIP-SHIP2 relatively efficiently ameliorated the reduced PKCλ activity caused by the chronic insulin treatment to 65.0±7.5% of the control level. A combination of rapamycin treatment and expression of ΔIP-SHIP2 more effectively restored the insulin-induced activation of PKCλ. In contrast to the results for the phosphorylation of Akt, the restoration of PKCλ activity was still partial, and was 75.2±4.1% of the control level. The partial amelioration of insulin-stimulated PKCλ activity after chronic insulin treatment was also seen with advanced overexpression of IRS-1 (Fig. 4a). The amount of PKCλ protein was not

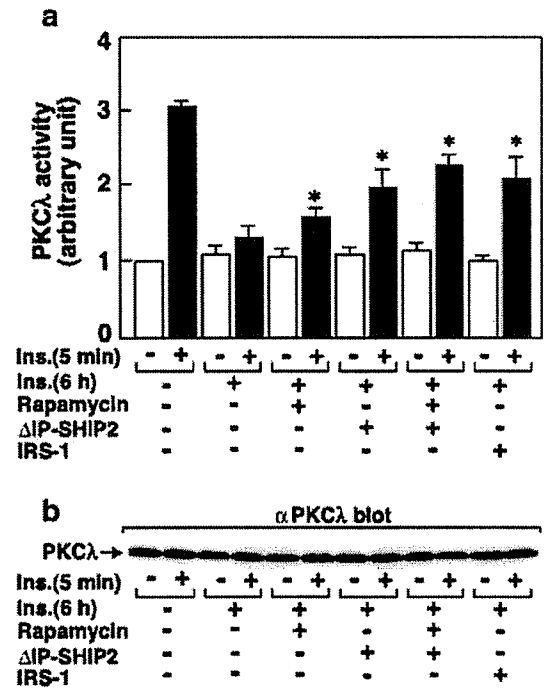

Fig. 4 Effect of ΔIP-SHIP2 and IRS-1 expression, and pretreatment with rapamycin, on insulin-induced activation of PKCλ after chronic insulin treatment. 3T3-L1 adipocytes were transfected with LacZ and ΔIP-SHIP2 at an m.o.i. of 40 pfu/cell, or IRS-1 at an m.o.i. of 10 pfu/cell. Serum-starved transfected cells were incubated with vehicle or 20 nmol/l rapamycin for 30 min, and treated with 17 nmol/l insulin for 6 h. The cells were washed with PBS, incubated in insulin-free medium for 30 min, and stimulated with 100 nmol/l insulin for 5 min. They were then lysed and immunoprecipitated with anti PKCλ antibody. Kinase reactions were conducted, and samples were fractionated by SDS-PAGE. **a** The radioactivity incorporated into substrates was determined with a Fuji BAS 2000 image analyser. Results are means ± SEM of three separate experiments; *$p<0.05$ versus insulin-stimulated PKCλ activity in LacZ-transfected control cells with chronic insulin treatment. **b** The cell lysates were separated by SDS-PAGE, and immunoblotted with anti-PKCλ antibody.

altered either by chronic insulin treatment, treatment with rapamycin, or expression of ΔIP-SHIP2 and IRS-1 (Fig. 4b).

Effect of ΔIP-SHIP2 and IRS-1 expression, and pretreatment with rapamycin, on insulin-induced 2-DOG uptake after chronic insulin treatment Since insulin-stimulated phosphorylation of Akt and PKCλ activity decreased by the chronic insulin treatment was ameliorated by rapamycin treatment and expression of ΔIP-SHIP2 and IRS-1, we next examined these effects on insulin stimulation of 2-DOG uptake (Fig. 5a). Again, insulin-induced 2-DOG uptake was markedly decreased to 25.6±5.2% after chronic insulin treatment. Pretreatment with rapamycin and expression of ΔIP-SHIP2 partially restored the decreased 2-DOG uptake to 47.5±3.7% and 54.4±4.1%, respectively, of the control level. Both rapamycin treatment and ΔIP-SHIP2 expression more efficiently ameliorated the reduced 2-DOG uptake to 69.2±4.4%. Advanced overexpression of IRS-1 also improved the reduced 2-DOG uptake to 69.7 ±2.5% of the control level. The amount of Glut4 protein was not altered either by chronic insulin treatment, treatment with rapamycin, or overexpression of ΔIP-SHIP2 and IRS-1 (Fig. 5b).

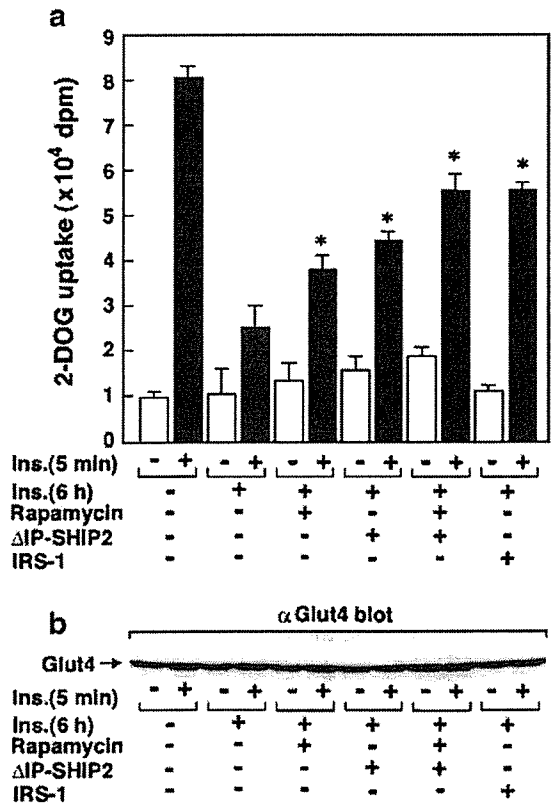

Fig. 5 Effect of ΔIP-SHIP2 and IRS-1 expression, and pretreatment with rapamycin, on insulin-induced 2-DOG uptake after chronic insulin treatment. 3T3-L1 adipocytes were transfected with LacZ and ΔIP-SHIP2 at an m.o.i. of 40 pfu/cell, or IRS-1 at an m.o.i. of 10 pfu/cell. Serum-starved transfected cells were incubated with vehicle or 20 nmol/l rapamycin for 30 min, and treated with 100 nmol/l insulin for 6 h. The cells were washed with PBS, incubated in insulin-free medium for 3 h, and washed again with PBS and incubated in glucose-free medium for another 30 min. After the cells had been stimulated with 10 nmol/l insulin for 5 min, 3.7 kBq of 2-[^{3}H]DOG was added for 3 min. The reaction was stopped by the addition of 10 μmol/l cytochalasin B. The cells were washed three times with PBS and solubilized with 0.2 mmol/l SDS–0.2 N NaOH. **a** The radioactivity incorporated into the cells was measured with a liquid scintillation counter. Results are means ± SEM of three separate experiments. *$p<0.05$ versus insulin-induced 2-DOG uptake in LacZ-transfected control cells with chronic insulin treatment. **b** The cell lysates were separated by SDS-PAGE and immunoblotted with anti-Glut4 antibody.

Discussion

Chronic insulin exposure is known to cause a subsequent insulin resistance, by reducing the level of IRS-1 via PI3-kinase and rapamycin-dependent pathways [17–21, 30, 31]. In fact, our results demonstrated that chronic insulin treatment induced a reduction in IRS-1 levels in a time-dependent manner. In addition to the impaired IRS-1–dependent signalling pathway, the present study showed increased amounts of SHIP2 following chronic insulin exposure. Since SHIP2 is the physiologically important negative regulator of insulin signalling with a fundamental impact on the state of insulin resistance [8–12], the increase in SHIP2 protein appears to be part of the novel molecular mechanism of insulin resistance caused by chronic insulin treatment. Because SHIP2 is translocated to the plasma membrane where it functions to hydrolyse PI(3,4,5)P3, the increase in the amount of SHIP2 protein in the plasma membrane preparation further supports the possible involvement of SHIP2 in insulin resistance in 3T3-L1 adipocytes [26].

We employed two approaches to ameliorate the decrease in IRS-1 levels caused by the chronic insulin treatment. As shown in Fig. 3, pretreatment with rapamycin prevented the mTOR-dependent proteosomal degradation of IRS-1 caused by the chronic insulin treatment. Overexpression of exogenous IRS-1 in advance normalized the decreased IRS-1 levels caused by the insulin treatment. On the other hand, endogenous SHIP2 function was efficiently inhibited by expression of the 5′-phosphatase defective dominant-negative SHIP2 (ΔIP-SHIP2) as shown in Fig. 2. These approaches would be useful for clarifying whether the rescue of insulin signalling at the level of IRS-1 and/or SHIP2 is effective in ameliorating insulin resistance caused by chronic insulin treatment. The decrease in the phosphorylation of Akt caused by the chronic insulin treatment was effectively ameliorated by either prevention of the decrease in IRS-1 by rapamycin treatment or advanced IRS-1 overexpression, or inhibition of endogenous SHIP2 function by expression of the dominant-negative SHIP2 (ΔIP-SHIP2). These results indicate that insulin-induced phosphorylation of Akt is closely associated with the IRS-1–mediated PI3-kinase pathway. In addition, the full input of insulin signal does not appear to be required for the sufficient phosphorylation of Akt, because amelioration of insulin signalling at the step involving IRS-1

or SHIP2 is sufficient for the efficient restoration of the phosphorylation of Akt.

Phosphorylation at both Thr^{308} and Ser^{473} is required for the full activation of Akt [8, 26–28]. In this context, our results showed that the rescue of IRS-1 levels by treatment with rapamycin and overexpression of IRS-1 in advance, and expression of the dominant-negative SHIP2 (ΔIP-SHIP2), efficiently ameliorated the decreased insulin-induced phosphorylation of Akt at both residues caused by the chronic insulin treatment. In contrast to the effective recovery of acute insulin stimulation of Akt phosphorylation, the recovery of acute insulin stimulation of PKCλ activation was only partial for both the restoration of IRS-1 levels and inhibition of SHIP2 function. Thus, pretreatment with rapamycin, advanced IRS-1 overexpression, and ΔIP-SHIP2 expression only partially ameliorated the insulin-induced activation of PKCλ to 49.8±3.8%, 67.2±8.5%, and 65.0±7.5%, respectively, of the control value. The rescue of the PKCλ activity was still partial with a combination of ΔIP-SHIP2 expression and rapamycin pretreatment (or IRS-1 expression—data not shown). Therefore, the insulin resistance caused by chronic treatment may also impair insulin signalling at the step important for PKCλ activation more directly in addition to the IRS-1–PI3-kinase pathway. It is possible that another insulin signalling system important for glucose uptake including the CAP–Cbl–TC10 pathway may be a candidate implicated in the signalling step, although further investigation is needed to clarify the issue [32, 33]. We can not rule out the possibility that full activation of the IRS-1–PI3-kinase pathway is required for the efficient activation of PKCλ, although resistance at the levels of IRS-1 and SHIP2 appears to be efficiently rescued by pretreatment with rapamycin and expression of ΔIP-SHIP2.

Interestingly, the decreased stimulation of 2-DOG uptake caused by chronic insulin treatment was only partly restored by the maintenance of IRS-1 levels by pretreatment with rapamycin or advanced overexpression of IRS-1, or expression of ΔIP-SHIP2 as shown in Fig. 5. These findings are consistent with the results of PKCλ activation, and not Akt activation. Although Akt and atypical PKC are downstream effectors of PI3-kinase strongly implicated in the metabolic actions of insulin, the relative importance of Akt versus atypical PKC in insulin-induced 2-DOG uptake is controversial [8, 22, 27–29, 34]. Our results indicate that PKCλ/ζ rather than Akt may be more closely linked to the insulin-stimulated glucose uptake and associated with the state of insulin resistance. It is unclear whether this difference between Akt and PKCλ activation in chronic insulin treatment reflects a small input of IRS-1–dependent insulin signalling sufficient for Akt activation, or whether factors other than IRS-1–dependent insulin signalling are involved in the impairment of PKCλ activation. In any event, our results indicate that PKCλ activity rather than Akt activity appears to be associated with the decreased glucose uptake caused by chronic insulin treatment. Regardless of the importance of PKCλ to the state of insulin resistance, overexpression of the constitutively active form of PKCλ did not completely rescue the decreased insulin-stimulated glucose uptake caused by the chronic insulin treatment (data not shown). Based on this observation, chronic insulin treatment appears to cause insulin resistance at multiple signalling steps including a step distal to the PKCλ activation leading to the glucose uptake. It is also possible that chronic insulin treatment impairs the glucose uptake involved in the Glut4 translocation system independent of insulin signalling as previously reported for the insulin resistance caused by dexamethasone treatment in 3T3-L1 adipocytes [23].

In summary, SHIP2 appears to participate in insulin resistance, at least in part, caused by chronic insulin treatment in 3T3-L1 adipocytes. In addition, (1) impaired early insulin signalling occurring mainly at IRS-1 for the PI3-kinase activation, (2) impaired insulin signalling for PKCλ activation, and (3) impaired glucose transport system may also be involved in the insulin resistance caused by chronic insulin treatment. Furthermore, the present study indicates that the inhibition of endogenous SHIP2 appears to be effective at ameliorating the insulin signal in a state of insulin resistance, and that the activity of PKCλ rather than Akt may be more closely associated with the decreased 2-DOG uptake caused by the chronic insulin treatment in 3T3-L1 adipocytes. Taken together, inhibition of the endogenous level and/or function of SHIP2 would be an important therapeutic target of insulin resistance in type 2 diabetes.

Acknowledgements This work was supported in part by a grant-in-aid for scientific research from the Japan Society for the Promotion of Science. We thank Dr Wataru Ogawa (Kobe University, Japan) for kindly providing the anti-PKCλ antibody and Dr Kazuyuki Hiratani (Toyama Medical and Pharmaceutical University, Japan) for technical assistance. T. Sasaoka and K. Fukui contributed equally to this work.

References

1. Rameh LE, Cantley LC (1999) The role of phosphoinositide 3-kinase lipid products in cell function. J Biol Chem 274:8347–8350
2. Cantley LC (2002) The phosphoinositide 3-kinase pathway. Science 296:1655–1657
3. Virkamäki A, Ueki K, Kahn CR (1999) Protein–protein interaction in insulin signaling and the molecular mechanisms of insulin resistance. J Clin Invest 103:931–943
4. Czech MP, Corvera S (1999) Signaling mechanisms that regulate glucose transport. J Biol Chem 274:1865–1868
5. Saltiel AR, Pessin JE (2002) Insulin signaling pathways in time and space. Trends Cell Biol 12:65–71
6. Pesesse X, Deleu S, De Smedt F, Drayer L, Erneux C (1997) Identification of a second SH2-domain-containing protein closely related to the phosphatidylinositol polyphosphate 5-phosphatase SHIP. Biochem Biophys Res Commun 239:697–700
7. Ishihara H, Sasaoka T, Hori H et al (1999) Molecular cloning of rat SH2-containing inositol phosphatase 2 (SHIP2) and its role in the regulation of insulin signaling. Biochem Biophys Res Commun 260:265–272
8. Wada T, Sasaoka T, Funaki M et al (2001) Overexpression of SH2-containing inositol phosphatase 2 results in negative regulation of insulin-induced metabolic actions in 3T3-L1 adipocytes via its 5′-phosphatase catalytic activity. Mol Cell Biol 21:1633–1646

9. Sasaoka T, Hori H, Wada T et al (2001) SH2-containing inositol phosphatase 2 negatively regulates insulin-induced glycogen synthesis in L6 myotubes. Diabetologia 44:1258–1267
10. Clement S, Krause U, Desmedt F et al (2001) The lipid phosphatase SHIP2 controls insulin sensitivity. Nature 409:92–97
11. Hori H, Sasaoka T, Ishihara H et al (2002) Association of SH2-containing inositol phosphatase 2 with the insulin resistance of diabetic db/db mice. Diabetes 51:2387–2394
12. Marion E, Kaisaki PJ, Pouillon V et al (2002) The gene INPPL1, encoding the lipid phosphatase SHIP2, is a candidate for type 2 diabetes in rat and man. Diabetes 51:2012–2017
13. Reaven GM (1988) Role of insulin resistance in human disease. Diabetes 37:1595–1607
14. DeFronzo RA, Ferrannini E (1991) Insulin resistance: a multifaceted syndrome responsible for NIDDM, obesity, hypertension, dyslipidemia, and atherosclerotic cardiovascular disease. Diabetes Care 14:173–194
15. Goalstone ML, Natarajan R, Standley PR et al (1998) Insulin potentiates platelet-derived growth factor action in vascular smooth muscle cells. Endocrinology 139:4067–4072
16. Rondinone CM, Wang L-M, Lonnroth P, Wesslau C, Pierce JH, Smith U (1997) Insulin receptor substrate (IRS) 1 is reduced and IRS-2 is the main docking protein for phosphatidylinositol 3-kinase in adipocytes from subjects with non-insulin-dependent diabetes mellitus. Proc Natl Acad Sci U S A 94:4171–4175
17. Ricort J-M, Tanti J-F, Van Obberghen E, Le Marchand-Brustel Y (1995) Alterations in insulin signalling pathway induced by prolonged insulin treatment of 3T3-L1 adipocytes. Diabetologia 38:1148–1156
18. Thomson MJ, Williams MG, Frost SC (1997) Development of insulin resistance in 3T3-L1 adipocytes. J Biol Chem 272: 7759–7764
19. Berg CE, Lavan BE, Rondinone CM (2002) Rapamycin partially prevents insulin resistance induced by chronic insulin treatment. Biochem Biophys Res Commun 293:1021–1027
20. Haruta T, Uno T, Kawahara J et al (2000) A rapamycin-sensitive pathway down-regulates insulin signaling via phosphorylation and proteasomal degradation of insulin receptor substrate-1. Mol Endocrinol 14:783–794
21. Takano A, Usui I, Haruta T et al (2001) Mammalian target of rapamycin pathway regulates insulin signaling via subcellular redistribution of insulin receptor substrate 1 and integrates nutritional signals and metabolic signals of insulin. Mol Cell Biol 21:5050–5062
22. Kotani K, Ogawa W, Matsumoto M et al (1998) Requirement of atypical protein kinase Cλ for insulin stimulation of glucose uptake but not for Akt activation in 3T3-L1 adipocytes. Mol Cell Biol 18:6971–6982
23. Sakoda H, Ogihara T, Anai M et al (2000) Dexamethazone-induced insulin resistance in 3T3-L1 adipocytes is due to inhibition of glucose transport rather than insulin signal transduction. Diabetes 49:1700–1708
24. Sun XJ, Goldberg JL, Qiao L, Mitchell JJ (2002) Insulin-induced insulin receptor substrate-1 degradation is mediated by the proteasome degradation pathway. Diabetes 48:1359–1364
25. Zhande R, Mitchell JJ, Wu J, Sun XJ (2002) Molecular mechanism of insulin-induced degradation of insulin receptor substrate 1. Mol Cell Biol 22:1016–1026
26. Ishihara H, Sasaoka T, Ishiki M et al (2002) Membrane localization of src homology 2-containing inositol 5′-phosphatase 2 via Shc association is required for the negative regulation of insulin signaling in rat1 fibroblasts overexpressing insulin receptors. Mol Endocrinol 16:2371–2381
27. Kitamura T, Ogawa W, Sakaue H et al (1998) Requirement for activation of the serine-threonine kinase Akt (protein kinase B) in insulin stimulation of protein synthesis but not of glucose transport. Mol Cell Biol 18:3708–3717
28. Wang Q, Somwar R, Bilan PJ et al (1999) Protein kinase B/Akt participates in Glut4 translocation by insulin in L6 myoblasts. Mol Cell Biol 19:4008–4018
29. Bandyopadhyay G, Standaert ML, Zhao L et al (1997) Activation of protein kinase C (α, β, and ζ) by insulin in 3T3/L1 cells: transfection studies suggest a role for PKC-ζ in glucose transport. J Biol Chem 272:2551–2558
30. Pessin JE, Saltiel AR (2000) Signaling pathways in insulin action: molecular targets of insulin resistance. J Clin Invest 106:165–169
31. Sykiotis GP, Papavassiliou AG (2001) Serine phosphorylation of insulin receptor substrate-1: a novel target for the reversal of insulin resistance. Mol Endocrinol 15:1864–1869
32. Baumann CA, Ribon V, Kanzaki M et al (2000) CAP defines a second signalling pathway required for insulin-stimulated glucose transport. Nature 407:202–207
33. Chiang S-H, Baumann CA, Kanzaki M et al (2001) Insulin-stimulated Glut4 translocation requires the CAP-dependent activation of TC10. Nature 410:944–948
34. Bandyopadhyay G, Kanoh Y, Sajan MP, Standaert ML, Farese RV (2000) Effects of adenoviral gene transfer of wild-type, constitutively active, and kinase-defective protein kinase C-λ on insulin-stimulated glucose transport in L6 myotubes. Endocrinology 141:4120–4127

JOURNAL OF CELLULAR PHYSIOLOGY 202:536–553 (2005)

PKC Mediates Cyclic Stretch-Induced Cardiac Hypertrophy Through Rho Family GTPases and Mitogen-Activated Protein Kinases in Cardiomyocytes

JING PAN,[1]* UGRA S. SINGH,[1] TOSHIYUKI TAKAHASHI,[1] YOSHITOMO OKA,[2] ANTS PALM-LEIS,[1] BRADLEY S. HERBELIN,[1] AND KENNETH M. BAKER[1]

[1]*Division of Molecular Cardiology, Cardiovascular Research Institute, The Texas A&M University System Health Science Center, College of Medicine, Temple, Texas*

[2]*Division of Molecular Metabolism and Diabetes, Department of Internal Medicine, Tohoku University Graduate School of Medicine, Sendai, Japan*

Signaling events, including Rho GTPases and protein kinase C (PKC), are involved in cardiac hypertrophy. However, the mechanisms by which these pathways cooperate during the hypertrophic process remain unclear. Using an in vitro cyclic stretch model with neonatal rat cardiomyocytes, we demonstrated that stretch-induced activation of RhoA, Rac1/Cdc42, and phosphorylation of Rho-guanine nucleotide dissociation inhibitor (GDI) were prevented by inhibition or depletion of PKC, using chelerythrine and phorbol 12-myristate 13-acetate, indicating that phorbol ester-sensitive PKC isozymes may be upstream regulators of Rho GTPases. Using adenoviral-mediated gene transfer of wild-type (WT) and dominant-negative (DN) mutants of PKCα and δ, we found that stretch-induced activation of Rho GTPases and phosphorylation of Rho-GDI were mainly regulated by PKCα. PKCδ was involved in regulation of the activation of Rac1. Stretch-induced increases in [^{3}H]-leucine incorporation, myofibrillar reorganization and cell size, were blocked by inhibition of Rho GTPases, or overexpression of DN PKCα and δ, suggesting that PKCα and δ are both required in stretch-induced hypertrophy, through Rho GTPases-mediated signaling pathways. The mechanism, whereby PKC and Rho GTPases regulate hypertrophy, was associated with mitogen-activated protein (MAP) kinases. Stretch-stimulated phosphorylation of MEK1/ERK1/2 and MKK4/JNK was inhibited by overexpression of DN PKCα and δ, and that of MKK3/p38 inhibited by DN PKCδ. The phosphorylation of ERK and JNK induced by overexpression of WT PKCα, and the phosphorylation of p38 induced by WT PKCδ, were regulated by Rho GTPases. This study represents the first evidence that PKCα and δ are important regulators in mediating activation of Rho GTPases and MAP kinases, in the cyclic stretch-induced hypertrophic process. J. Cell. Physiol. 202: 536–553, 2005. © 2004 Wiley-Liss, Inc.

Mechanical stretch is a major initiating factor for cardiac hypertrophy (Cooper et al., 1985; Komuro et al., 1990; Sadoshima et al., 1992), which evokes various intracellular signaling pathways, such as Rho family GTPases, protein kinase C (PKC), tyrosine kinases, and mitogen-activated protein (MAP) kinase cascades (Sadoshima and Izumo, 1993; Yamazaki et al., 1993; Pan et al., 1999). Although various intracellular signals have been identified, little is known about the potential interplay between these signaling pathways.

The Rho family GTPases, which include RhoA, Rac1, and Cdc42, have been implicated in the regulation of a number of biological processes including cell morphology, motility, adhesion, and growth (Cox et al., 1997; Hall, 1998; Nobes and Hall, 1999). The major function of Rho GTPases is to regulate the assembly and the organization of the actin cytoskeleton (Ridley and Hall, 1992). Cardiac hypertrophy is associated with cell growth and changes in the cytoskeleton and myofibrillar apparatus. Reports indicate that RhoA, Rac1, and Cdc42 are involved in modulating cardiac hypertrophy (Aoki et al., 1998; Pracyk et al., 1998; Aikawa et al., 1999; Nagai et al., 2003). However, the mechanism of

Contract grant sponsor: National Institutes of Health; Contract grant numbers: HL-44883, HL-58439.

*Correspondence to: Jing Pan, Assistant Professor, Cardiovascular Research Institute, The Texas A&M University System Health Science Center, 1901 South 1st Street, Building 205, Temple, TX 76504. E-mail: jpan@medicine.tamu.edu

Received 7 January 2004; Accepted 14 May 2004

DOI: 10.1002/jcp.20151

activation of Rho GTPases has not been well characterized. RhoA activates several protein kinases, including protein kinase N (PKN) and Rho kinases (ROCK2 and ROCK1) (Ishizaki et al., 1996; Watanabe et al., 1996). It has been demonstrated that both PKN and Rho kinase are involved in the Rho-induced hypertrophic response (Morissette et al., 2000; Yanazume et al., 2002). Rac1 promotes activation of ERK, JNK, and p38-MAPK via PAK1 (Zhang et al., 1995; Nosaka et al., 2001; Schmitz et al., 2001). In cardiac myocytes, Rac1 cooperates with c-Raf to promote ERK activation and ANF expression (Clerk et al., 2001).

Rho GTPases cycle between a GDP-bound inactive form and a GTP-bound active form, a process regulated by guanine nucleotide exchange factors (GEFs), which catalyze the exchange of GDP for GTP (Cerione and Zheng, 1996); GTPase activating proteins, which stimulate hydrolysis of GTP to GDP (Lamarche and Hall, 1994); and guanine nucleotide dissociation inhibitors (GDIs), which inhibit the dissociation of GDP from Rho GTPases (Fukumoto et al., 1990). The dissociation of GDI is a prerequisite for membrane association and activation of Rho GTPases by GEFs (Bokoch et al., 1994). The mechanism of the release of Rho-GDI from Rho GTPases remains unclear; but likely involves phosphatidylinositols and the ERM family of proteins (ezrin, radixin, and moesin) (Faure et al., 1999; Mammoto et al., 2000). The structure of Rho-GDI contains sequences for phosphorylation by serine/threonine kinases, which raises the possibility that phosphorylation of GDI promotes release of GDI from Rho GTPases (Olofsson, 1999). It has been reported that PKC regulates thrombin-induced activation of RhoA, through phosphorylation of Rho-GDI, suggesting that GDI phosphorylation may be required for activation of Rho GTPases (Mehta et al., 2001).

PKC consists of a family of serine/threonine kinases, which regulate intracellular signaling and mediate cell proliferation, differentiation, and rearrangement of the cytoskeleton (Nishizuka, 1992; Keenan and Kelleher, 1998). PKC isoforms are divided into three subgroups as follows: the "conventional" (cPKC) α, βI, βII, and γ; the "novel"(nPKC) δ, ε, η, and θ; and the "atypical"(aPKC) ζ, λ, and ι isozymes. Using transgenic mice and adenoviral-mediated overexpression, studies have demonstrated that PKCα and ε are involved in agonist-induced hypertrophic gene expression and growth (Mende et al., 1999; Takeishi et al., 2000; Strait et al., 2001; Braz et al., 2002; Kerkela et al., 2002). The role of PKCδ in cardiac hypertrophy has not been well characterized. Reports have shown that PKCδ expression/activation is increased in cardiac hypertrophy in vivo (Strait and Samarel, 2000; Chen et al., 2001; Braun et al., 2002, 2003), and may also be involved in apoptosis (Chen et al., 2001; Simonis et al., 2002). Mechanical stretch-induced cardiac hypertrophy is also regulated by PKC (Kashiwagi et al., 1998; Seko et al., 1999). However, direct evidence implicating a specific PKC isozyme, as a dominant regulator of stretch-induced hypertrophy, is lacking. PKC and Rho GTPases both have effects on the actin cytoskeleton and activation of MAPK pathways (Ridley and Hall, 1992; Hall, 1998; Keenan and Kelleher, 1998; Toker, 1998). Studies that have directly linked PKC and Rho GTPases signaling suggest significant crosstalk between these two pathways (Nozu et al., 1999; Coghlan et al., 2000; Slater et al., 2001). The targets and signaling pathways shared by Rho GTPases and PKC directed our focus in determining whether these two pathways cooperate in mediating the hypertrophic process.

In the present study, we demonstrated that cyclic stretch-induced activation of Rho GTPases is mediated by PKC (especially PKCα and δ), which by phosphorylating Rho-GDI, regulates the activation of Rho GTPases, and MAP kinase pathways. Our data suggest that the interconnectivity of PKC, Rho GTPases, and MAP kinases has an important role in cyclic stretch-induced cardiac hypertrophy.

MATERIALS AND METHODS

Materials

Monoclonal antibodies against RhoA, Cdc42, polyclonal antibodies against PKCα, ε, δ, ζ, Rho-GDI, ERK1/2, JNK1, p38MAPK, MBP, c-jun, ATF-2, actin and GST-ATF2, c-jun were from Santa Cruz Biotechnology (San Diego, CA). A monoclonal antibody against Rac1 was from Transduction Laboratories (San Jose, CA). Specific phospho-MEK1, MEK3, MEK4, ERK1/2, JNK, and p38 antibodies were from Cell Signaling Technology (Beverly, MA). C3 exoenzyme, Toxin B, and chelerythrine chloride were from Calbiochem (San Diego, CA). [γ-^{32}P]ATP, [α-^{32}P]dCTP, ^{32}P, and [^{3}H]-Leucine were from Perkin Elmer Life Sciences (Boston, MA). Rat ANP and c-fos plasmid was kindly provided by Dr. Fukuda (Keio University, Tokyo, Japan). Other reagents were purchased from Sigma Chemical Co (St. Louis, MO).

Cell culture of cardiomyocytes

Neonatal cardiomyocytes were prepared from the ventricles of 1-day-old Sprague–Dawley rats, as previously described (Kodama et al., 1997) and were cultured in 10% horse serum and 5% fetal bovine serum for 24 h at a density of 1.5×10^5 cells/cm^2 in laminin-coated six-well BioFlex culture plates (Flex cell International Corporation, PA). After 48 h, serum-starved cells were subjected to cyclic stretch using the Flexcell 3000 Strain Unit. The vacuum produced a 15% elongation on the flexible bottom membranes at a frequency of 60 cycles/min. Culture plates not subjected to cyclic stretch were used as controls.

Adenovirus generation

The replication-defective adenovirus-encoding wild-type (WT) or dominant negative mutants of PKCα and δ were gifts from Dr. Yoshitomo Oka (Sendai, Japan). The dominant negative PKCα (AdPKCαdn) and PKCδ (AdPKCδdn) cDNAs consisted of a lysine to arginine mutation in the ATP binding domain at amino acid position 368 and 376, respectively. Each recombinant adenovirus was plaque purified, and amplified using HEK293 cells. The multiplicity of viral infection (moi) for each virus was determined by dilution assay in HEK293 cells. Cardiomyocytes were infected with each adenovirus at a moi of 50 pfu for 6 h at 37°C. Subsequently, the cells were cultured in serum-free DMEM/F12 media for an additional 24 h before treatments or analysis.

Rho, Rac1, and Cdc42 activity assays

The small G protein affinity binding assays were performed using glutathione *S*-transferase (GST) fusion proteins with the Rho binding domain from rotekin (GST-RBD, for RhoA), with the Rac1 and Cdc42 interactive binding domain from PAK1 (GST-PBD, for Rac1/Cdc42), according to the manufacturer's protocol (Upstate Biotechnology, Charlottesville, VA). In brief, myocytes were lysed, and an equal volume of cell lysates was incubated with GST-RBD, GST-PBD, or GST beads (negative control). The samples were separated on SDS–PAGE. Activated RhoA, Rac1, and Cdc42 were detected by Western blotting, with antibodies against RhoA, Rac1, or Cdc42. Another set of equal amount of lysates was Western blotted with corresponding antibodies, to normalize the activated Rho GTPases in different samples. Scanning densitometry was used for semiquantitative analysis of the data.

In vitro kinase assay

ERK, JNK, and p38 MAPK activity was examined as previously described (Yamazaki et al., 1993). In brief, cardiomyocytes were lysed in buffer containing 20 mM Tris-HCl, pH 7.5, 150 mM NaCl, 1 mM EDTA, 1 mM EGTA, 1% Triton X-100, 2.5 mM sodium pyrophosphate, 1 mM β-glycerophosphate, 1 mM sodium vanadate, 10 μg/ml leupeptin and aprotinin, and 1 mM phenylmethylsulfonyl fluoride. The lysate was sedimented at 15,000*g* for 15 min at 4°C, and used for immunoprecipitation of p38, JNK1, or ERK 1/2. Immunoprecipitates were washed three times with the lysis buffer and two times with kinase buffer (25 mM HEPES, pH 7.4, 5 mM β-glycerophosphate, 2 mM dithiothreitol, and 10 mM $MgCl_2$) and resuspended in 40 μl of kinase buffer containing 4 μg of GST-ATF-2, GST-c-jun, or 20 μg of MBP, 50 μM ATP, and 10 μCi of [γ-^{32}P]ATP. The reaction mixture was incubated at 30°C for 20 min, terminated by the addition of 5× Laemmli's sample buffer. Samples were subjected to electrophoresis on SDS–PAGE, transferred to nitrocellulose membrane, and exposed to X-ray films. Loading differences were determined by blotting the membrane with anti-ERK, JNK1, p38, and MBP, c-jun, or ATF-2 antibodies.

Phosphorylation of Rho-GDI

Phosphorylation of Rho-GDI was performed using an in vivo labeling method (Mehta et al., 2001). In brief, serum-starved myocytes were labeled with 300 μCi/ml ^{32}P for 4 h in phosphate-free medium, and subjected to stretch for the indicated times. Cell lysates were immunoprecipitated with Rho-GDI or normal rabbit IgG (negative control) antibody. The phosphorylation of Rho-GDI was visualized by autoradiography. The blots were Western blotted with anti-Rho-GDI antibody to verify an equal amount of the protein in each sample. In vitro phosphorylation of GST-GDI was performed by incubating GST-GDI fusion proteins (Cytoskeleton, Inc., Denver, CO) with immunocomplexes of PKCα, δ, ζ, or ε obtained after immunoprecipitation of cell lysates with respective PKC antibodies or normal IgG (negative control), as previously described (Jain et al., 1999).

Subcellular fractionation and PKC translocation assay

Subcellular fractionation was performed as previously described (Strait and Samarel, 2000). Briefly, cardiomyocytes were sonicated in homogenization buffer (25 mM Tris-HCl, pH 7.5, 4 mM EGTA, 2 mM EDTA, 5 mM DTT, 1 mM PMSF, 10 μg/ml aprotinin and leupeptin), and sedimented (100,000*g* for 60 min, 4°C), the supernatant fraction was saved as the cytosolic fraction. The pellet was resuspended in homogenization buffer with the addition of 1% Triton X-100. The sample was sonicated and sedimented again at 100,000*g* for 30 min at 4°C, the supernate was saved as the particulate sample.

Western blotting

Cardiomyocytes were lysed in lysis buffer. Equal amounts of extracted proteins were separated on 10% SDS–PAGE, transferred to nitrocellulose membrane, and the Western blots probed with antibodies specific for PKCα, δ, or the phosphorylated forms of MEK1, MEK3, MEK4, ERK1/2, JNK, or p38 MAPK. Membranes were reprobed with antibodies recognizing unphosphorylated forms of MAP kinases to confirm equal loading. Primary antibody binding was detected with horseradish-peroxidase-conjugated goat anti-mouse or goat anti-rabbit secondary antibody and visualized by chemiluminescence (NEN Life Science, Boston, MA).

Leucine incorporation

Serum starved cardiomyocytes were subjected to cyclic stretch for 24 h. [^{3}H]-Leucine (1 μCi/ml) was added 4 h before harvest. The total radioactivity of incorporated [^{3}H]-Leucine into proteins was measured by liquid scintillation counting, as described previously (Yamazaki et al., 1995).

RNA isolation and Northern blot analysis

Total RNA was isolated using TRIzol reagent. Total RNA (20 μg) was separated on 1% MOPS-formaldehyde-agarose gel, and Northern blots were performed, as described previously (Manabe et al., 1999).

Immunocytochemistry

After 24 h of cyclic stretch, cardiomyocytes were fixed in 3.7% paraformaldehyde, and permeabilized with 0.3% Triton X-100. Cells were incubated with Texas Red-X phalloidin (1:40), or PKCα and δ antibodies (1:400). For characterization of PKC distribution, cells were further incubated with anti-rabbit FITC-conjugated secondary antibody (1:400, Sigma-Aldrich, St. Louis, MO). Immunostained cardiomyocytes were viewed by fluorescence microscopy. Quantitation of cell surface area was performed on actin-stained cardiomyocytes.

Statistical analysis

Data expressed as the mean ± SEM. Statistical differences were determined using a Student's *t*-test ($P < 0.05$).

RESULTS

Cyclic stretch induces activation of Rho GTPases in cardiomyocytes

By using a GST-RBD and GST-PBD pulldown assay, we observed that cyclic stretch induced a significant (sixfold) increase in RhoA-GTP, with maximal stimulation within 1–10 min. The binding of RhoA to GST-RBD was sustained at a higher level at 60 min (Fig. 1A,C). In contrast, stretch induced a rapid activation (about sevenfold) of Rac1 and Cdc42 in 1 min, which decreased to a basal level in 30 min (Fig. 1A,C). As a negative control, cell lysates prepared from stretched cells were incubated with GST beads, and activation of RhoA and Rac1 were examined. As shown in Figure 1B, we could not detect pulldown of GTP-RhoA and GTP-Rac1 (using GST beads), demonstrating the specificity of GST-RBD and GST-PBD assays.

Rho GTPases are involved in the cyclic stretch-induced hypertrophic responses

Cardiomyocytes were subjected to cyclic stretch for 24 h in the presence or absence of Toxin B or C3 exoenzyme (C3). Toxin B inactivates Rho family GTPases, but not Ras family proteins (Hofmann et al., 1997). C3 inactivates RhoA by ADP-ribosylating RhoA within the effector domain. It does not contain a binding or transfer component and therefore cannot efficiently permeate into the cell interior to access its enzymatic target. By using the liposome formulation lipofectamine, C3 can be efficiently introduced into cells (Borbiev et al., 2000). Cardiomyocytes were pretreated with lipofectamine (10 μg/ml) for 45 min, and exposed to C3 (5 μg/ml) overnight before subjecting to cyclic stretch for 24 h. Cyclic stretch induced a marked increase in cell size and an increase in both the staining intensity and the organization of the actin fibers in the cell cytoplasm (Fig. 2A). The increased cell size was inhibited by pretreatment with Toxin B and C3 (Fig. 2B). The myofibrillar reorganization was disrupted with a decreased intensity of actin immunostaining in Toxin B and C3 treated cells (Fig. 2A). Toxin B and C3 alone had no effect on the myocardial cell phenotype. Cyclic stretch promoted [^{3}H]-leucine incorporation, with an 80% increase observed, compared to control (Fig. 2C). Toxin B and C3 significantly inhibited the increase in leucine incorporation (70% and 65%, respectively). Both inhibitors had minimal effects on the basal level. Northern blot analysis demonstrated that stretch-induced expression of c-fos and ANP was blocked in Toxin B and C3 treated cells (Fig. 2D,E). These results suggest that Rho GTPases are required in cyclic stretch-induced cardiac hypertrophy.

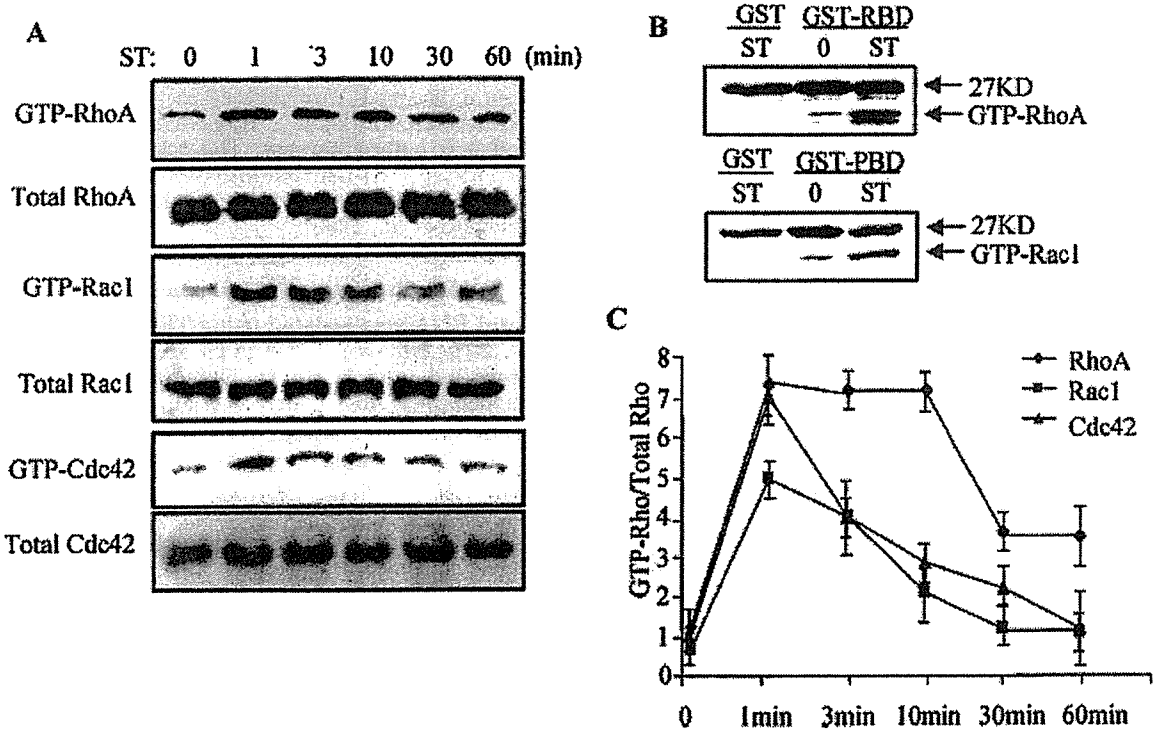

Fig. 1. Cyclic stretch induces activation of Rho GTPases. A: Cardiomyocytes were subjected to cyclic stretch (15% elongation, 60 cycle/min) for the times indicated. GTP-RhoA, GTP-Rac1, and GTP-Cdc42 were pulled down and detected by immunoblotting with anti-RhoA, -Rac1, and Cdc42 antibody, respectively. RhoA activity is indicated by the amount of RBD-bound RhoA normalized to the amount of RhoA in whole cell lysates; Rac1/Cdc42 activity is indicated by the amount of PBD-bound Rac1/or Cdc42 normalized to the amount of Rac1 or Cdc42 in whole cell lysates. B: Cardiomyocytes were subjected to cyclic stretch for 1 min, and the cell lysates were precipitated with GST-RBD, GST-PBD, or GST beads. The activation of RhoA and Rac1 was determined as in (A). GTP-RhoA, GTP-Rac1, and GTP-Cdc42 were quantified by scanning densitometry and were expressed relative to total proteins. Results are the mean ± SEM for three separate experiments (C).

Rho GTPases mediate cyclic stretch-induced activation of MAP Kinases

To further elucidate the downstream signaling pathways associated with the activated Rho GTPases, we determined the involvement of MAP Kinase pathways. Using an in vitro kinase assay, we demonstrated that ERK1/2, JNK, and p38MAPK were activated by cyclic stretch (Fig. 3A). ERK and JNK were activated at 5 min, and peaked at 15 min. The activation of p38 was observed at 2 min, with a maximum activation at 15 min. Stretch-induced activation of JNK and p38 was strongly inhibited, and that of ERK partially inhibited, by Toxin B (Fig. 3B, left part, and Fig. 3C). C3 significantly inhibited the activation of ERK and p38, and partially inhibited the activation of JNK. The membranes reprobed with antibody against ERK1/2, JNK1, or p38 and antibody against kinase substrates (MBP, c-jun, and ATF-2) showed an equal amount of protein in different samples. These results indicated that RhoA and Rac1/Cdc42 were differentially involved in mediating the activation of MAP kinases.

PKC regulates cyclic stretch-induced activation of Rho GTPases

To determine the role of PKC in cyclic stretch-mediated activation of Rho GTPases, chelerythrine

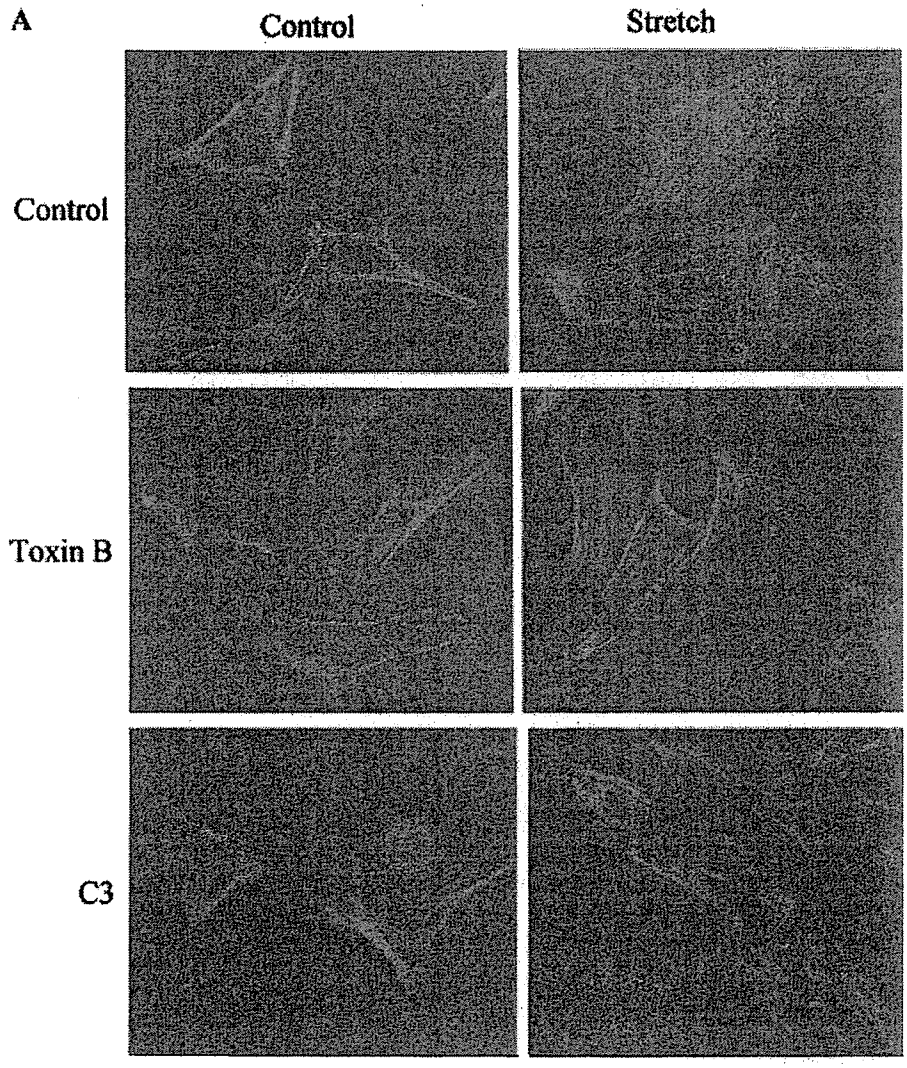

Fig. 2. Rho GTPases are involved in stretch-induced hypertrophic responses. **A:** Serum-starved cardiomyocytes were subjected to cyclic stretch for 24 h in the presence and absence of Toxin B (10 ng/ml) and C3 exoenzyme (5 μg/ml, overnight pretreatment, C3). Immunofluorescence was performed with Texas Red phalloidin antibody. **B:** Phalloidin-stained cells were imaged and cell surface areas calculated with the *Image J* Program (n = 100 cells each). $^{*}P < 0.001$ versus control; $^{\#}P < 0.001$ versus stretch. **C:** [^{3}H]-leucine (1 μCi/ml) was added 4 h before harvest. The total radioactivity of incorporated [^{3}H]-leucine into proteins was measured by liquid scintillation counting. Each bar represents the mean ± SEM of six separate experiments. $^{*}P < 0.05$ versus control and $^{\#}P < 0.05$ versus stretch. **D:** Cardiomyocytes were subjected to stretch for 30 min in the presence or absence of Toxin B and C3. Total RNA was extracted, and Northern blot was performed as described under Materials and Methods. **E:** Cardiomyocytes were subjected to stretch for 24 h in the presence or absence of Toxin B and C3. Total RNA was extracted, and Northern blot was performed.

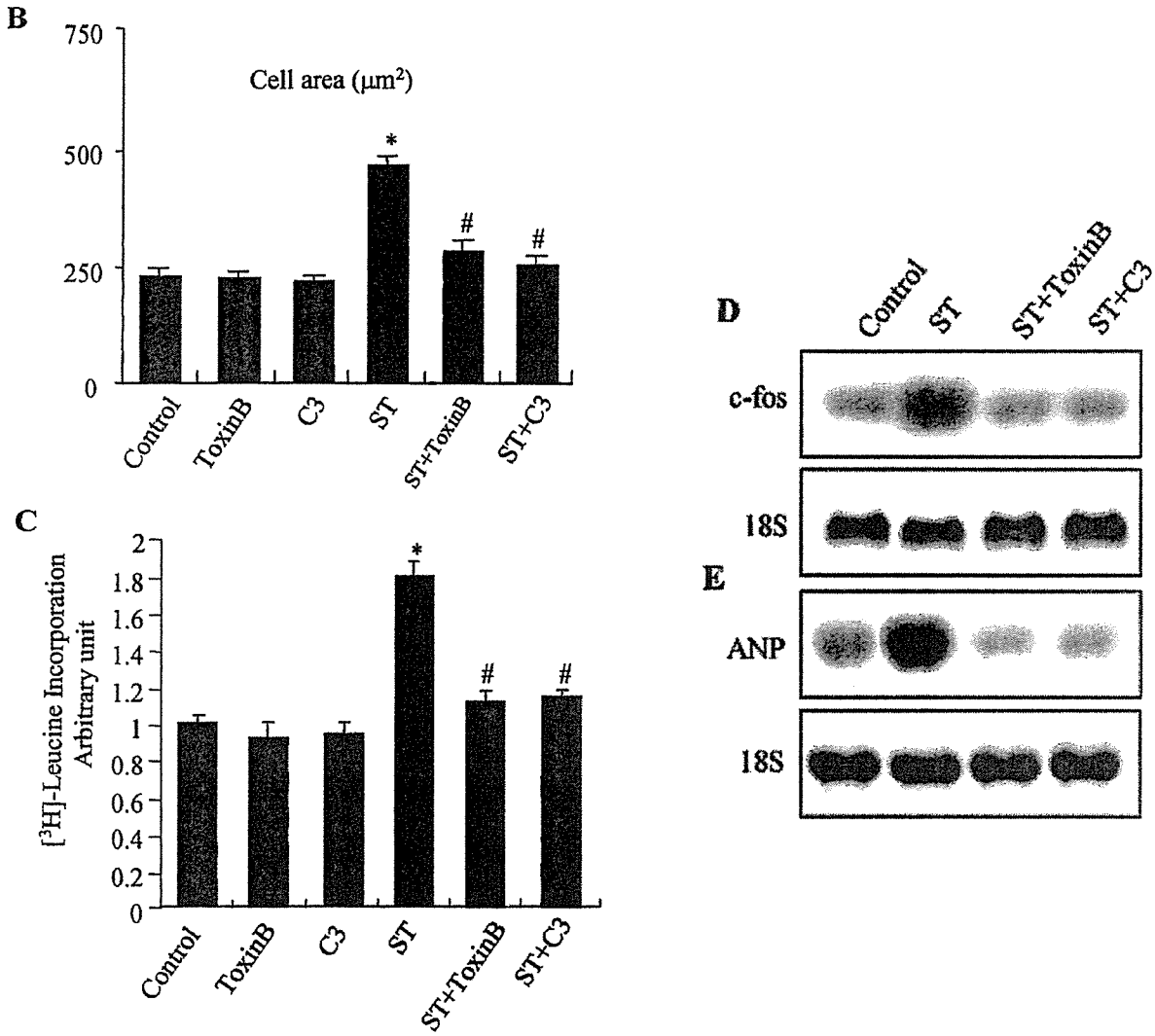

Fig. 2. (*Continued*)

chloride, a specific, but non-isozyme-selective PKC inhibitor was used. Cyclic stretch-induced activation of RhoA, and Rac1/Cdc42 was blocked by chelerythrine, indicating that PKC is an upstream regulator of Rho GTPases (Fig. 4A). We further determined whether the involved PKC isozymes were phorbol ester-sensitive, by depleting conventional and novel PKC isozymes using PMA (when applied chronically, it downregulates the expression of conventional and novel PKCs) (Szallasi et al., 1994). Overnight pretreatment of cardiomyocytes with PMA inhibited stretch-induced activation of Rho GTPases (Fig. 4A). PMA and chelerythrine alone had no effect on the activation of RhoA, Rac1, and Cdc42. To further understand the role of PKC activation in regulating Rho GTPases activation, we used PMA, as a direct activator of PKC. Cardiomyocytes were treated with PMA for 1–60 min, and the activation of Rho GTPases was determined. As shown in Figure 4B, PMA stimulation induced rapid activation of RhoA, Rac1, and Cdc42, which returned to basal level at 30 min. These data suggested that stretch-induced activation of Rho GTPases was regulated by phorbol ester-sensitive PKC isozymes.

PKC regulates cyclic stretch-induced phosphorylation of Rho-GDI

The dissociation of Rho-GDI is a prerequisite for membrane association and activation of Rho GTPases by GEFs (Bokoch et al., 1994). Rho-GDI phosphorylation/dephosphorylation has been implicated in regulation of the dissociation of the Rho GTPases/Rho-GDI complex (Bourmeyster and Vignais, 1996; Gorvel et al., 1998; Mehta et al., 2001). Using an in vivo labeling method, we observed that Rho-GDI was rapidly phosphorylated by cyclic stretch at 1 min, and returned to the basal level at 10 min, consistent with the activation of Rho GTPases (Fig. 5A). As a negative control, cell lysates from stretched cells were incubated with normal rabbit IgG, and the

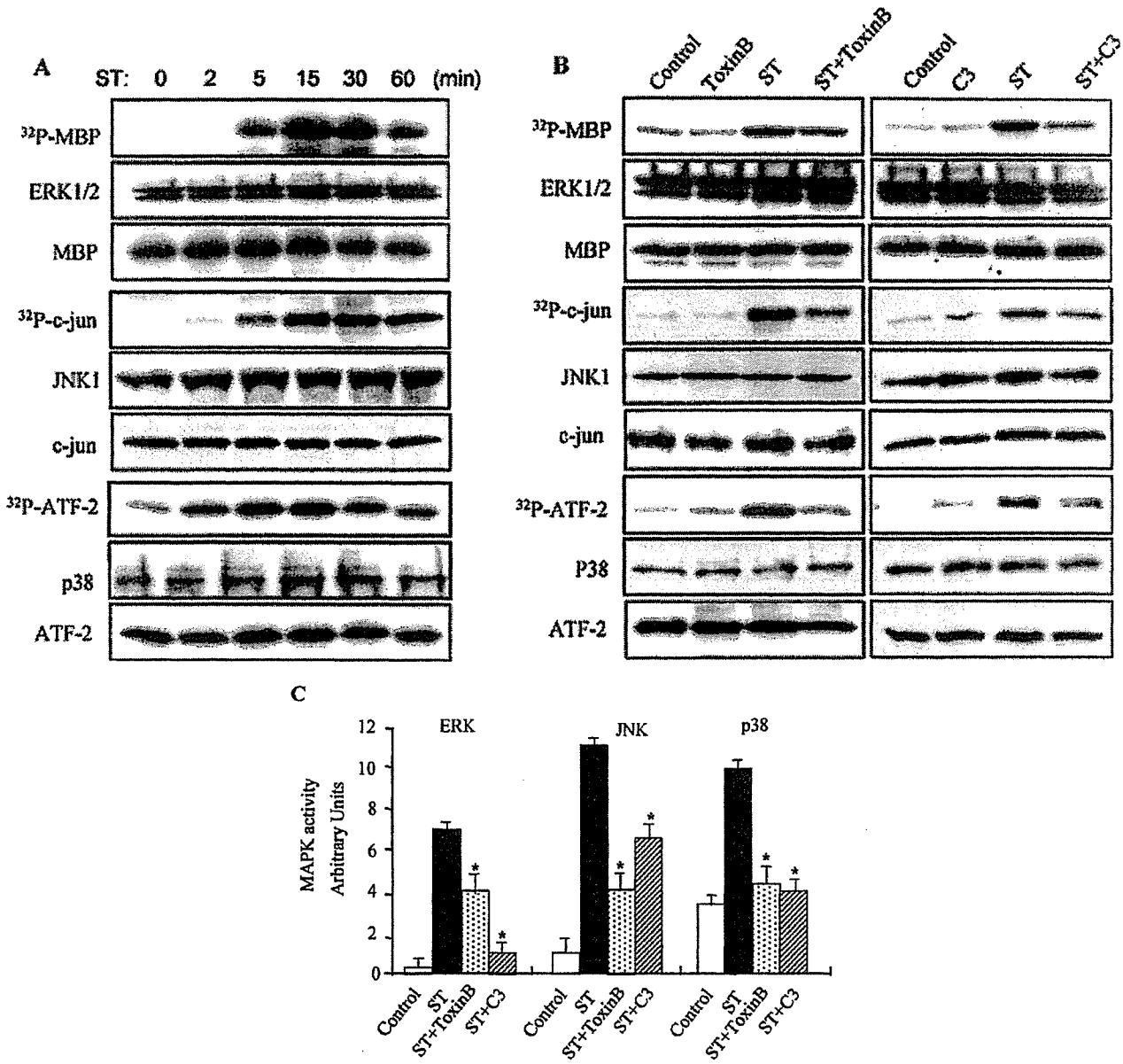

Fig. 3. Rho GTPase regulates cyclic stretch-induced activation of MAP kinases. A: Serum-starved cardiomyocytes were subjected to cyclic stretch for the times indicated. Cell lysates were used for immunoprecipitation of ERK, JNK1, and p38MAPK. A kinase assay was performed by adding 20 μg of myelin basic protein, 4μg of c-Jun or GST-ATF-2, respectively, and10 μCi of [γ-^{32}P] ATP. The samples were electrophoresed, transferred to nitrocellulose membrane, and exposed to X-ray films. The activity of ERK1/2, JNK, and p38MAPK was determined by autoradiography. The membranes were Western blotted with antibodies against ERK1/2, JNK p38, and corresponding kinase substrates, to verify an equal amount of protein in each sample. B: Cardiomyocytes were pretreated with or without Toxin B (10 ng/ml, 1 h) and C3 (5 μg/ml, overnight), then subjected to cyclic stretch for 15 min. The activity of ERK, JNK, and p38MAPK were determined as described above. C: Scanning densitometry was used for semiquantitative analysis of the data. Results are means ± SEM for three separate experiments. *$P < 0.05$ versus cyclic stretch.

in vivo phosphorylation of Rho-GDI was determined. As shown in Figure 5B, no phosphorylation of Rho-GDI was detected (left 2 lanes). Inhibition of PKC by chelerythrine or depletion of PKC by PMA, attenuated stretch-induced phosphorylation of Rho-GDI (Fig. 5C), indicating that phorbol-sensitive PKC isozymes are involved. We further determined whether PKC directly phosphorylated Rho-GDI in vitro, using GST-GDI as a substrate. GST-GDI was modestly phosphorylated by PKCα and δ in unstretched myocytes; but the phosphorylation significantly increased following cyclic stretch. Under similar conditions, PKCζ and ε failed to induce phosphorylation of GST-GDI (Fig. 5D). These results indicated that PKCα and δ were the major regulators in

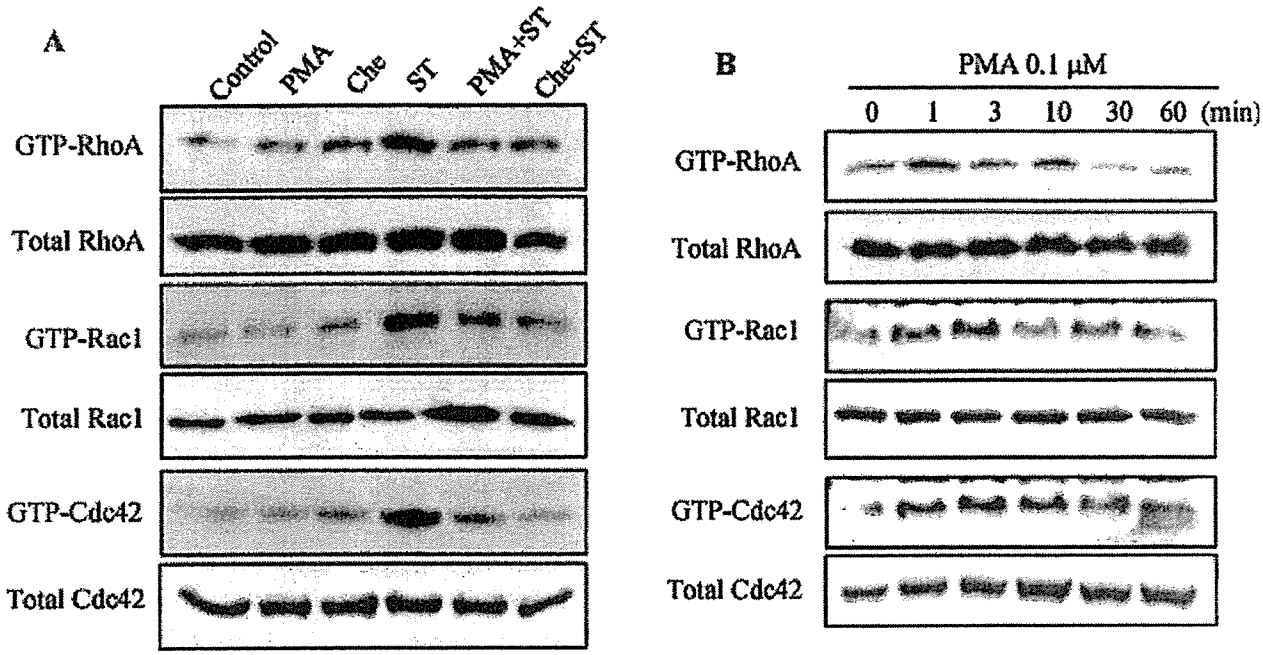

Fig. 4. PKC regulates stretch-induced activation of Rho GTPases. A: Cardiomyocytes were pretreated with or without chelerythrine (Che, 10 μM) for 30 min, or PMA (1 μM, overnight). After 1 min of stretching, Rho GTPases activity was assayed as described in Figure 1. B: Cardiomyocytes were exposed to PMA (0.1 μM) at the indicated times. Rho GTPase activity was assayed. Data are representative of three independent experiments.

mediating the phosphorylation of Rho-GDI. Another set of cell lysates were incubated with normal rabbit IgG, and in vitro kinase assay was performed to serve as a negative control (last part).

Subcellular localization of PKCα and δ

To determine the role of PKCα and δ in the regulation of cardiomyocyte growth and activation of Rho GTPases, the adenoviral-mediated gene transfer of WT and dominant-negative (DN) mutant of PKCα and δ was performed. Western blot analysis showed that the level of PKCα and δ overexpression was dose dependently increased after adenovirus infection (Fig. 6A). To verify the translocation of adenoviral-mediated overexpression of PKCα and δ in cardiomyocytes, cell membrane (particulate) and cytosolic (soluble) protein extracts were prepared and subjected to Western blotting. As shown in Figure 6B, endogenous PKCα and δ expression was predominantly located in the cytosolic fraction. AdPKCαWT and AdPKCδWT overexpression specifically increased the total PKC localization to the membrane fraction, while AdPKCαDN and AdPKCδDN overexpression increased total PKC localization to the cytosolic fraction. No crosstalk was observed between these two isozymes. To further characterize the subcellular localization of PKCα and δ, immunocytochemistry was performed. Overexpression of AdPKCαWT and AdPKCδWT demonstrated a diffuse distribution in cardiomyocytes; however, a significant concentration was observed surrounding the nucleus in AdPKCδWT infected cardiomyocytes. After 30 min of cyclic stretch stimulation, PKCα and δ demonstrated a distinct redistribution pattern (Fig. 6C). AdPKCαWT showed a localized perinuclear expression pattern, and AdPKCδWT redistributed into the nucleus. In contrast, overexpressing AdPKCαDN and AdPKCδDN blocked the redistribution of each PKC isozymes induced by cyclic stretch (Fig. 6C). In control virus AdLacZ infected myocytes, faint PKCα and δ antibody reactivity was observed in a diffuse pattern, which was consistent with the localization observed in WT overexpressing cells.

PKCα and δ differentially regulate the activation of Rho GTPases and phosphorylation of Rho-GDI

To determine the role of PKCα and δ in regulation of the activation of Rho GTPases and phosphorylation of Rho-GDI, cardiomyocytes were infected with adenoviral-mediated PKCα and δ mutants, and subjected to stretch for 1 min. Overexpression of AdPKCαDN blocked stretch-induced activation of RhoA and Rac1 (Fig. 7A), while AdPKCδDN overexpression inhibited stretch-induced activation of Rac1, and had no effect on stretch-induced activation of RhoA. However, the basal activation of RhoA was significantly increased in AdPKCδDN infected cardiomyocytes. Overexpression of AdPKCδWT inhibited the basal activation of RhoA, and mildly inhibited stretch-induced activation of RhoA. Stretch-induced phosphorylation of Rho-GDI was blocked by overexpression of AdPKCαDN, which is consistent with the regulation of Rho GTPases by PKCα (Fig. 7C). Overexpression of AdPKCδDN did not prevent the phosphorylation of Rho-GDI.

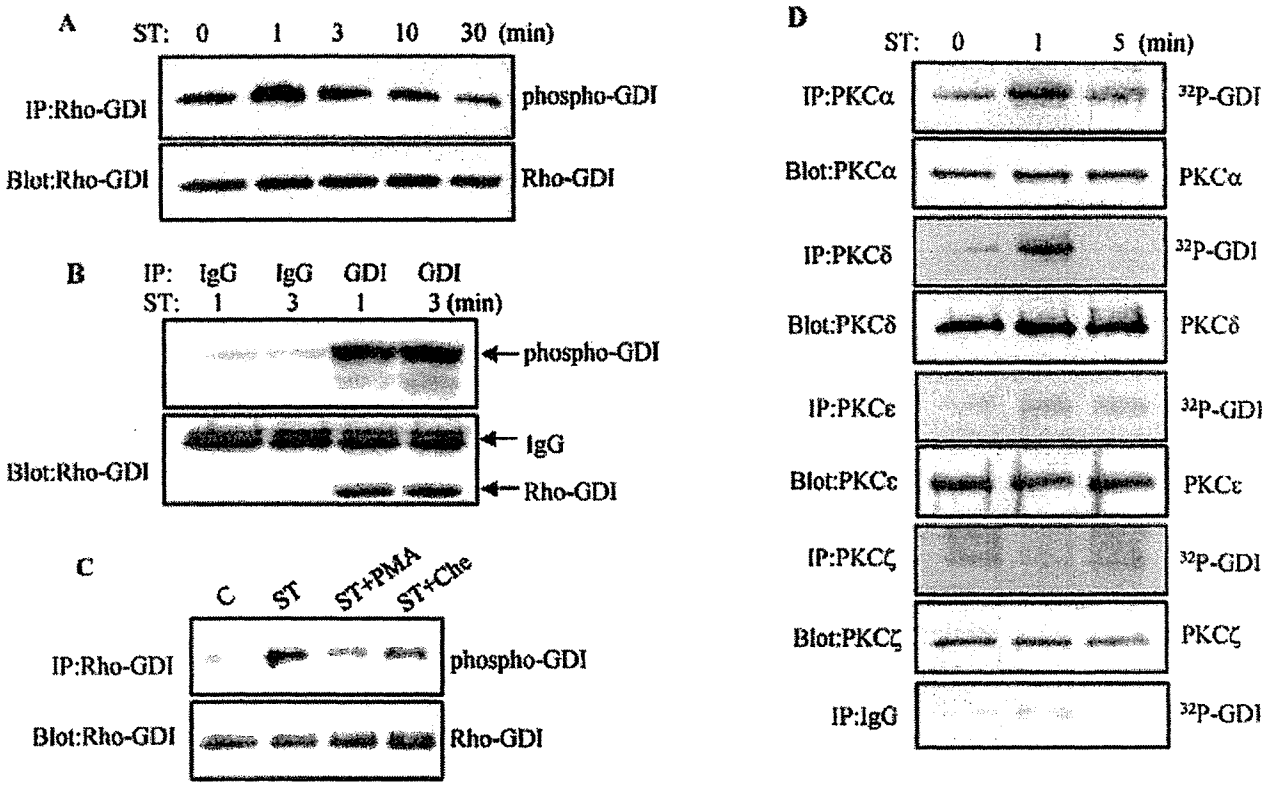

Fig. 5. PKC regulates stretch-induced Rho-GDI phosphorylation. A: Cardiomyocytes were subjected to stretch for the indicated times. Phosphorylation of Rho-GDI was determined as described under Materials and Methods. B: Cell lysates from stretched cells were immunoprecipitated with normal rabbit IgG (negative control) and Rho-GDI, phosphorylation of Rho-GDI was determined. C: Cardiomyocytes were pretreated with or without chelerythrine (Che, 10 μM) for 30 min, or PMA (1 μM, overnight). Phosphorylation of Rho-GDI was determined following 1 min of cyclic stretch. D: In vitro Rho-GDI phosphorylation. After stretching, cardiomyocytes were lysed to immunoprecipitate PKCα, δ, ζ, ε, or normal rabbit IgG (negative control, last part) as described under Materials and Methods. A kinase assay was performed using GST-GDI as a substrate. GDI phosphorylation was determined by autoradiography.

PKCα and δ are involved in cyclic stretch-induced cardiac hypertrophy

We have shown that stretch-activated Rho GTPases were required in the hypertrophic process (Fig. 2), and that the activation of Rho GTPases was differentially regulated by PKCα and δ (Fig. 7). Using adenoviral-mediated PKCα and δ mutants, we determined whether PKCα and δ were involved in stretch-induced cardiac hypertrophy. Overexpression of AdPKCαWT, but not AdPKCδWT, induced significant myofibrillar reorganization, increases in cell size and [^{3}H]-leucine incorporation (Fig. 8A–C). These data are consistent with previous studies (Braz et al., 2002), indicating that PKCα may be a unique inducer of cardiac hypertrophy. Cyclic stretch-induced increases in cell size and [^{3}H]-leucine incorporation were blocked by overexpression of AdPKCαDN and AdPKCδDN, and stretch-induced myofibrillar reorganization was also disrupted by AdPKCαDN and AdPKCδDN (Fig. 8A–C), suggesting that both PKCα and δ were required in cyclic stretch-induced cardiac hypertrophy.

PKCα and δ differentially regulate the activation of MEK/MAP kinase cascades

It has been reported that there is crosstalk between PKC and MAP kinase pathways in cardiomyocytes (Rohde et al., 2000; Heidkamp et al., 2001; Braz et al., 2002; Kerkela et al., 2002). To address the signaling mechanism, whereby PKC mediates stretch-induced hypertrophy, the activation of MAP kinases and their upstream regulator MAP kinase kinases (MKKs), in cardiomyocytes overexpressing PKCα and δ, was determined. Overexpression of AdPKCαWT induced phosphorylation of MEK1, MKK4, ERK1/2, and JNK, but not MKK3 and p38. In contrast, AdPKCδWT overexpression induced phosphorylation of MKK3 and p38, but had no effect on phosphorylation of MEK1, MKK4, ERK1/2, and JNK (Fig. 9A,B). Overexpression of AdPKCαWT and AdPKCδWT had no effect on the expression level of MEKs and MAPKs as demonstrated by Western blot using antibodies against normal MEKs and MAPKs. Another set of samples was Western blotted with actin antibody, to verify the equal amount of protein in each